AUGUST 15, 2016 VOLUME 64 NUMBER 16 ITPRED (ISSN 1053-587X)

REGULAR PAPERS

(Contents Continued on Page 4097)

IEEE TRANSACTIONS ON SIGNAL PROCESSING (ISSN 1053-587X) is published semimonthly by the Institute of Electrical and Electronics Engineers, Inc. Responsibility for the contents rests upon the authors and not upon the IEEE, the Society/Council, or its members. **IEEE Corporate Office:** 3 Park Avenue, 17th Floor, New York, NY 10016-5997. **IEEE Operations Center:** 445 Hoes Lane, Piscataway, NJ 08854-4141. **NJ Telephone:** +1 732 981 0060. **Price/Publication Information**: Individual copies: IEEE Members $39.00 (first copy only), nonmembers $663.00 per copy. (Note: Postage and handling charge not included.) Member and nonmember subscription prices available upon request. **Postmaster:** Send address changes to IEEE TRANSACTIONS ON SIGNAL PROCESSING, IEEE, 445 Hoes Lane, Piscataway, NJ 08854-4141. GST Registration No. 125634188. CPC Sales Agreement #40013087. Return undeliverable Canada addresses to: Pitney Bowes IMEX, P.O. Box 4332, Stanton Rd., Toronto, ON M5W 3J4, Canada.

(Contents Continued from Page 4096)

About the Cover: The cover depicts the determinant of FIM as a function of θ_2 and θ_3 with $\theta_1 = -60^\circ$ and maxima indicated with '+' for: (a) $\sigma_1 = \sigma_2 = \sigma_3 = 1$ (maxima occur at $\{\theta_2^*, \theta_3^*\} = \{60^\circ, 60^\circ\}$, $\{60^\circ, -60^\circ\}$ and $\{-60^\circ, 60^\circ\}$), (b) $\sigma_1 = 1$, $\sigma_2 = \sigma_3 = 0.5$ (maxima occur at $\{\theta_2^*, \theta_3^*\} = \{60^\circ, -60^\circ\}$ and $\{-60^\circ, 60^\circ\}$), and (c) $\sigma_1 = 1$, $\sigma_2 = 2$ and $\sigma_3 = 3$ (maximum occurs at $\{\theta_2^*, \theta_3^*\} = \{60^\circ, 60^\circ\}$) as presented in Fig. 5 of the paper "Optimal Geometry Analysis for Multistatic TOA Localization" by Nguyen and Doğançay on page 4180.

Oblique Projection Based Enumeration of Mixed Noncoherent and Coherent Narrowband Signals

Hao Tao, Jingmin Xin, *Senior Member, IEEE*, Jiasong Wang, Nanning Zheng, *Fellow, IEEE*, and Akira Sano, *Member, IEEE*

***Abstract*—In many application scenarios, the signals impinging on the array of sensors comprise the noncoherent (uncorrelated and/or partially correlated) signals and the coherent signals with several groups due to multipath propagation. In this paper, we consider the problem of estimating the number of noncoherent narrowband signals and that of coherent narrowband signals with multiple groups impinging on a planar sensor array composed of two parallel uniform linear arrays (ULAs), and an oblique projection based enumerator for the mixed signals (OPEMS) is proposed by utilizing the QR decomposition based ratio criterion (QRRC) for rank determination of a matrix. In the OPEMS, the number of noncoherent signals and that of coherent signals in each group are estimated separately, where only the elevation angles of noncoherent signals are estimated to isolate the coherent signals from the noncoherent ones, and the computationally intensive and time-consuming eigendecomposition procedure is avoided. The consistency of the proposed OPEMS is analyzed, and its effectiveness is verified through numerical examples.**

***Index Terms*—Detection of the number of signals, direction-of-arrival estimation, eigendecomposition, multipath propagation environment, oblique projection, QR decomposition.**

I. Introduction

DETECTION of the number of multiple signals impinging on an array of sensors and estimation of their direction-of-arrivals (DOAs) from the noisy measurements are two essentially important problems in array signal processing (cf. [1], [2]). Most of high-resolution subspace-based one-dimensional (1-D) DOA (i.e., azimuth angle) or 2-D DOA (i.e., elevation and azimuth angles) estimation methods with/without eigendecomposition (e.g., [3]–[16]) require the number of incident signals, and their performance is strongly dependent on the successful number determination of the incident signals (i.e., enumeration). Numerous enumeration methods were proposed from different perspective in the literature (e.g., [17]–[37]), and they can be broadly classified into two categories: separable detection methods and joint detection-estimation methods [2], where the DOA estimation is not required in the former, while the number of signals and the DOAs of all incident signals are estimated simultaneously in the latter.

In many application scenarios, multipath propagation is usually encountered due to various reflections caused by reflectors and scatterers (see, e.g., [1], [2] and references therein), and consequently the signals impinging on the array is a mixture of the noncoherent (uncorrelated and/or partially correlated) signals and the coherent (i.e., full correlated) signals with several groups (cf. [10]–[12], [29], [38]), where the rank of the noiseless array covariance matrix (i.e., the dimension of signal subspace) becomes less than the number of all incident signals. Although some aforementioned separable detection methods and joint detection-estimation methods (e.g., [25]–[37]) were proposed for the coherent signals, all of them can only estimate the total number of mixed signals, while the number of noncoherent signals and the numbers of coherent signals in each group can not be estimated separately. To the best of our knowledge, two separable detection methods [39], [41] were studied for the mixed noncoherent signals and coherent signals in the literature of array processing. With the aid of the (forward/backward) spatial smoothing (SS) preprocessing technique [42]–[44] and the information theoretic criteria such as the Akaike information criterion (AIC) or the minimum description length (MDL) [17], the smoothed rank profile (SRP) test [39] and its modification [40] were developed to estimate the number of noncoherent signals and the numbers of coherent signals in each group with the so-called SRP, which is defined as the rank profile of a telescoping series of matrices obtained by averaging smaller and smaller principal diagonal submatrices of the array covariance matrix, but its detection performance generally degrades, when the signal-to-noise ratio (SNR) is low and/or the number of snapshots is small. The eigenvalue-threshold method [41] requires the selection of a judiciously chosen threshold, which is not easy without any *a priori* knowledge in the case of a finite number of snapshots. Furthermore, almost all of the separable detection methods and the joint detection-estimation methods aforementioned involve the eigendecomposition procedure, which is computationally burdensome and time-consuming (cf. [45]–[47]), and hence it makes their real-time implementation be difficult, especially when the number of sensors is large (e.g., [9], [30], [48]–[52]). Additionally we proposed an enumeration method for the mixed signals [53], but it was applicable only for the case of a mixed uncorrelated signals and coherent signals with one group.

The array geometric configurations can be exploited to develop computationally efficient direction estimation and enumeration methods (cf. [54]). Some planar sensor arrays

Manuscript received December 28, 2015; accepted March 10, 2016. Date of publication March 31, 2016; date of current version July 05, 2016. The associate editor coordinating the review of this paper and approving it for publication was Prof. Adel Belouchrani. This work was supported in part by the National Natural Science Foundation of China under Grants 61172162 and 61231018, the Programme of Introducing Talents of Discipline to Universities under Grant B13043, and the Specialized Research Fund for the Doctoral Program of Higher Education of China under Grant 20130201110016.

H. Tao was with the National Engineering Laboratory of Visual Information Processing and Applications and the Institute of Artificial Intelligence and Robotics, Xi'an Jiaotong University, Xi'an 710049, China. He is now with the China Ship Development and Design Center, Wuhan 430064, China.

J. Xin and N. Zheng are with the National Engineering Laboratory of Visual Information Processing Applications and the Institute of Artificial Intelligence and Robotics, Xi'an Jiaotong University, Xi'an 710049, China (e-mail: jxin@mail.xjtu.edu.cn; nnzheng@mail.xjtu.edu.cn).

J. Wang is with the State Key Laboratory of Astronautic Dynamics, Xi'an 710043, China.

A. Sano is with the Department of System Design Engineering, Keio University, Yokohama 223-8522, Japan (e-mail: sano@sd.keio.ac.jp).

Digital Object Identifier 10.1109/TSP.2016.2548994

structured by two or more uniform linear arrays (ULAs) with simple and specified geometry configurations have advantages in geometric configuration and implementation compared with conventional uniform rectangular planar array, and they have received considerable attention in direction estimation (e.g., [55]–[59], [15], [16] and references therein), where the complicated 2-D DOA estimation with pair-matching can be accomplished with reduced computational complexity by applying most 1-D subspace-based estimation methods. Especially we proposed an oblique projection based approach for 2-D direction estimation (OPADE) for the mixed noncoherent and coherent narrowband signals impinging upon two parallel ULAs [16], but the numbers of the noncoherent and coherent signals were assumed to be known *a priori*.

Therefore the purpose of this paper is to investigate a new enumeration method for the noncoherent narrowband signals and the coherent narrowband signals with multiple groups impinging upon two parallel ULAs. By applying the oblique projection to isolate the coherent signals from the noncoherent ones (cf. [60]) and exploiting forward/backward (subarray) averaging to decorrelate the signals coherency and to enhance the performance of parameter estimation (e.g., [42]–[44], [61]), we propose an oblique projection based enumerator for the mixed signals (OPEMS), where the eigendecomposition procedure is avoided. Firstly, the number of noncoherent signals and the number of coherent groups are estimated from the rank of a cross-covariance matrix and that of a combined matrix with a QR decomposition based ratio criterion (QRRC), where the QR decomposition is a useful alternative to the eigendecomposition, because it requires much lesser computational load than the latter and is more amenable to real-time implementation (cf. [45]–[47], [62]–[65], [49], [50]). Then, the elevation angles of noncoherent signals are estimated from the cross-covariance matrix of two ULAs through a linear operator, and an oblique projector is obtained by using these estimated elevation angles. Finally, by using the estimated oblique projector to isolate the coherent signals from the noncoherent ones, a telescoping series of matrices which only contain the information of coherent signals are constructed, and the numbers of coherent signals in each group (i.e., the source coherency structure) are determined from the ranks of these telescoping matrices. Thus the proposed OPEMS can resolve more incident signals, because the number of noncoherent signals and that of coherent ones in each group are determined separately. Furthermore, the OPEMS is a companion to the previously proposed OPADE for 2-D DOA estimation of the mixed noncoherent and coherent signals [16]. The consistency of the proposed OPEMS is analyzed, and the simulation results demonstrate that the OPEMS has good performance in detecting the closely-spaced noncoherent and coherent signals, when the number of snapshots is small and/or the SNR is low.

II. Problem Statement

A. Basic Notation

The following notational conventions are used throughout this paper: the italic letters, lower-case boldface letters and capital boldface letters indicate the scalars, column vectors and matrices, and $\boldsymbol{I}_M$ and $\boldsymbol{J}_M$ are the $M \times M$ identity matrix and $M \times M$ exchange matrix, which has unity elements along the counter-diagonal and zeros elsewhere, while $E\{\cdot\}, (\cdot)^*, (\cdot)^T$, and $(\cdot)^H$ denote the statistical expectation, complex conjugate, transposition, and Hermitian transposition respectively. Further $\mathrm{diag}(\cdot), \mathrm{blkdiag}(\cdot), \min(\cdot)$, and $\rho(\cdot)$ represent the diagonal matrix operator, block diagonal matrix operator, minimum operator, and the rank of the bracketed matrix, while $\mathcal{R}(\cdot)$ and $\mathcal{N}(\cdot)$ signify the range space or the null space of the bracketed matrix. Additionally $\otimes, \oplus$, and $\cap$ indicate the Kronecker product, the direct sum operator and the intersection operator, while $\mathrm{tr}(\cdot)$ and $\mathrm{vec}(\cdot)$ denote the trace of the bracketed matrix and a matrix operation stacking the columns of the bracketed matrix one under the other to form a single column beginning with the leftmost column, while $\hat{x}$ means the estimate of x.

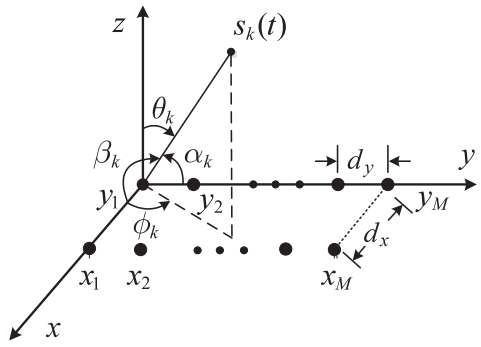

Fig. 1. The geometrical configuration of the planar array consisting of two parallel ULAs.

B. Data Model

As shown in Fig. 1, we consider a planar array consisting of two parallel ULAs placed in the x-y plane and assume that K narrowband signals $\{s_k(t)\}_{k=1}^{K}$ are a mixture of K_n noncoherent (including uncorrelated and partially correlated) and K_c coherent narrowband signals impinging on the array from far-field along 2-D distinct elevation-azimuth angles $\{(\alpha_k, \beta_k)\}$, where $K = K_n + K_c$. Each ULA has M omnidirectional sensors with spacing d_y, and the interelement spacing between two ULAs is d_x, while α_k and β_k are measured relatively to the y axis or the x axis as depicted in Fig. 1 (e.g., [2], [56], [58], [16]), and these angles and the conventional elevation and azimuth angles $\{(\theta_k, \phi_k)\}$ satisfy the simple relations that $\cos\alpha_k = \sin\theta_k \sin\phi_k$ and $\cos\beta_k = \sin\theta_k \cos\phi_k$ (cf. (Remark 2, [16])).

Herein we suppose that $\{s_k(t)\}_{k=1}^{K_n}$ and $\{s_k(t)\}_{k=K_n+1}^{K}$ are the noncoherent signals and coherent ones and these K_c coherent signals consist of P groups from P statistically independent sources $\{s_{cp}(t)\}_{p=1}^{P}$ under the flat-fading multipath propagation (cf. [10]–[12], [43]), where the pth group has K_p coherent signals with its kth signal expressed as $s_{p,k}(t) = \eta_{p,k} s_{cp}(t)$, in which $\eta_{p,k}$ is complex attenuation coefficient relative to $s_{cp}(t)$ with $\eta_{p,k} \neq 0$ and $\eta_{p,1} = 1$ for $p = 1, 2, \ldots, P$ and $k = 1, 2, \ldots, K_p$, while the corresponding elevation and azimuth angles are re-expressed as $(\alpha_{p,k}, \beta_{p,k})$, and $K_c = \sum_{p=1}^{P} K_p \geq 2P$. Hence the incident signals (including the noncoherent and coherent signals) can be expressed in a compact form as [16]

$$\boldsymbol{s}(t) \triangleq [s_1(t), s_2(t), \ldots, s_K(t)]^T = \Gamma \overline{\boldsymbol{s}}(t) \qquad (1)$$

where

$$\Gamma = \mathrm{blkdiag}\left(\boldsymbol{I}_{K_n}, \Lambda\right), \Lambda \triangleq \mathrm{blkdiag}\left(\boldsymbol{\eta}_1, \boldsymbol{\eta}_2, \ldots, \boldsymbol{\eta}_P\right),$$

$$\boldsymbol{\eta}_p \triangleq \left[\eta_{p,1}, \eta_{p,2}, \ldots, \eta_{p,K_p}\right]^T, \overline{\boldsymbol{s}}(t) \triangleq \left[\boldsymbol{s}_n^T(t), \overline{\boldsymbol{s}}_c^T(t)\right]^T,$$

$$\boldsymbol{s}_n(t) \triangleq \left[s_1(t), s_2(t), \ldots, s_{K_n}(t)\right]^T,$$

and $\overline{\boldsymbol{s}}_c(t) \triangleq [s_{c1}(t), s_{c2}(t), \cdots, s_{cP}(t)]^T$, while $\overline{\boldsymbol{s}}(t)$ is the "compressed" signal vector composed of the K_n noncoherent signals (i.e., $\boldsymbol{s}_n(t)$) and the P coherent source signals (i.e., $\overline{\boldsymbol{s}}_c(t)$). Thus, the received signals vectors of two ULAs can be expressed as [16]

$$\boldsymbol{x}(t) \triangleq \left[x_1(t), x_2(t), \cdots, x_M(t)\right]^T = \boldsymbol{A}\boldsymbol{D}\Gamma\overline{\boldsymbol{s}}(t) + \boldsymbol{w}_x(t) \tag{2}$$

$$\boldsymbol{y}(t) \triangleq \left[y_1(t), y_2(t), \cdots, y_M(t)\right]^T = \overline{\boldsymbol{A}}\overline{\boldsymbol{s}}(t) + \boldsymbol{w}_y(t) \tag{3}$$

where $\boldsymbol{A} \triangleq [\boldsymbol{A}_n, \boldsymbol{A}_c]$, $\boldsymbol{A}_n$ and $\boldsymbol{A}_c$ are the Vandermonde array response matrices corresponding to the K_n noncoherent signals and the K_c coherent signals and their columns are given by

$$\boldsymbol{a}(\alpha_k) \triangleq \left[1, e^{j\tau(\alpha_k)}, \ldots, e^{j(M-1)\tau(\alpha_k)}\right]^T,$$

$$\boldsymbol{a}(\alpha_{p,k}) \triangleq \left[1, e^{j\tau(\alpha_{p,k})}, \ldots, e^{j(M-1)\tau(\alpha_{p,k})}\right]^T,$$

$$\tau(\alpha_k) \triangleq 2\pi d_y \cos\alpha_k/\lambda, \tau(\alpha_{p,k}) \triangleq 2\pi d_y \cos\alpha_{p,k}/\lambda,$$

$$\boldsymbol{D} \triangleq \mathrm{diag}(e^{j\gamma(\beta_1)}, e^{j\gamma(\beta_2)}, \ldots, e^{j\gamma(\beta_{K_n})}, e^{j\gamma(\beta_{1,1})}, e^{j\gamma(\beta_{1,2})}, \ldots, e^{j\gamma(\beta_{P,K_P})}),$$

$$\gamma(\beta_k) \triangleq 2\pi d_x \cos\beta_k/\lambda, \gamma(\beta_{p,k}) \triangleq 2\pi d_x \cos\beta_{p,k}/\lambda,$$

$$\bar{\boldsymbol{A}} \triangleq [\boldsymbol{A}_n, \bar{\boldsymbol{A}}_c]$$

and $\overline{\boldsymbol{A}}_c \triangleq \boldsymbol{A}_c\Lambda$, while $\boldsymbol{w}_y(t)$ and $\boldsymbol{w}_x(t)$ are the vectors of additive noises, and λ is the wavelength.

In this paper, we make the following basic assumptions on the data model.

1) The array is calibrated, and the array response matrix $\boldsymbol{A}$ and the generalized one $\overline{\boldsymbol{A}}$ have full rank and are unambiguous.
2) The noncoherent signals $\{s_k(t)\}_{k=1}^{K_n}$ and the coherent source signals $\{s_{cp}(t)\}_{p=1}^{P}$ are temporally complex Gaussian random processes with zero mean, while the coherent source signals are uncorrelated with each other, and they are uncorrelated with the noncoherent signals.
3) The additive noises $\{w_{y_i}(t)\}$ and $\{w_{x_i}(t)\}$ are temporally and spatially complex white Gaussian random processes with zero-mean and the covariance matrices $E\{\boldsymbol{w}_y(n)\boldsymbol{w}_y^H(t)\} = E\{\boldsymbol{w}_x(n)\boldsymbol{w}_x^H(t)\} = \sigma^2\boldsymbol{I}_M\delta_{n,t}$ and $E\{\boldsymbol{w}_y(n)\boldsymbol{w}_y^T(t)\} = E\{\boldsymbol{w}_x(n)\boldsymbol{w}_x^T(t)\} = \boldsymbol{O}_{M\times M}, \forall n, t$, and they are uncorrelated with each other, i.e., $E\{\boldsymbol{w}_y(n)\boldsymbol{w}_x^H(t)\} = \boldsymbol{O}_{M\times M}, \forall n, t$. Additionally these additive noises are uncorrelated with the incident signals.
4) The numbers of noncoherent signals, coherent signals, coherent signals in each group and coherent groups $K_n, K_c, \{K_p\}$ and P satisfy the relation $M \geq \max\{K_n + 2P, K_c + L\} + 1$ (see Remark 6 for details), where L is the highest degree of coherency present (i.e., the maximum number of signals that are coherent with one another) defined by $L \triangleq \max\{K_p\}$ for $p = 1, 2, \ldots, P$.

Under the basic assumptions, from (2) and (3), we can obtain the cross-covariance matrix $\boldsymbol{R}_{yx}$ as

$$\boldsymbol{R}_{yx} \triangleq E\left\{\boldsymbol{y}(t)\boldsymbol{x}^H(t)\right\} = \overline{\boldsymbol{A}}\boldsymbol{R}_{\bar{s}}\Gamma^H\boldsymbol{D}^H\boldsymbol{A}^H \tag{4}$$

where $\boldsymbol{R}_{\bar{s}} \triangleq E\{\bar{\boldsymbol{s}}(t)\bar{\boldsymbol{s}}^H(t)\} = \mathrm{blkdiag}(\boldsymbol{R}_n, \boldsymbol{R}_{\bar{c}})$, $\boldsymbol{R}_n \triangleq E\{\boldsymbol{s}_n(t)\cdot\boldsymbol{s}_n^H(t)\}$, and $\boldsymbol{R}_{\bar{c}} \triangleq E\{\bar{\boldsymbol{s}}_c(t)\bar{\boldsymbol{s}}_c^H(t)\}$, while $\boldsymbol{R}_n$ is a nonsingular covariance matrix of noncoherent signals, and $\boldsymbol{R}_{\bar{c}}$ is a diagonal covariance matrix of the coherent source signals. Since $\overline{\boldsymbol{A}}$ is full rank and the rank of $\boldsymbol{R}_{\bar{s}}$ is given by $\rho(\boldsymbol{R}_{\bar{s}}) = K_n + P < K$, clearly $\rho(\boldsymbol{R}_{yx}) = K_n + P$, and neither the number of noncoherent signals K_n nor the numbers of coherent signals $\{K_p\}_{p=1}^{P}$ in each group can be determined from $\boldsymbol{R}_{yx}$ directly.

In the following, we concentrate on the problem of estimating the number of noncoherent signals K_n and the numbers of coherent signals in each group $\{K_p\}_{p=1}^{P}$ from finite noisy array data $\{\boldsymbol{y}(t)\}_{t=1}^{N_t}$ and $\{\boldsymbol{x}(t)\}_{t=1}^{N_t}$, where N_t is the number of snapshots.

Remark 1: When the additive noises $\{w_{y_i}(t)\}$ and $\{w_{x_i}(t)\}$ are not temporally and spatially complex white Gaussian random processes, but they are uncorrelated with each other, i.e., $E\{\boldsymbol{w}_y(n)\boldsymbol{w}_x^H(t)\} = \boldsymbol{O}_{M\times M}, \forall n, t$, the proposed OPEMS is still valid. □

III. Oblique Projection Based Enumerator for Mixed Signals—OPEMS

Here we develop a method called OPEMS for determining the numbers of noncoherent and coherent signals with multiple groups and the source coherency structure by exploiting the special configuration of two parallel ULAs and the oblique projection technique. The proposed OPEMS includes three stages: 1) detection of the number of noncoherent signals, 2) 1-D estimation of the elevation angles of noncoherent signals and estimation of oblique projector, and 3) detection of the numbers of coherent signals in each group with a telescoping series of matrices obtained from the projected array data, where the eigendecomposition is not required.

A. Enumeration of Noncoherent Signals and Coherent Groups

From (4), we obtain an outer-product matrix Ψ of $\boldsymbol{R}_{yx}$ as

$$\Psi \triangleq \boldsymbol{R}_{yx}\boldsymbol{R}_{yx}^H = \overline{\boldsymbol{A}}\boldsymbol{R}_{\bar{s}}\Gamma^H\boldsymbol{D}^H\boldsymbol{A}^H\boldsymbol{A}\boldsymbol{D}\Gamma\boldsymbol{R}_{\bar{s}}\overline{\boldsymbol{A}}^H. \tag{5}$$

We easily find $\rho(\Psi) = \rho(\boldsymbol{R}_{yx}) = K_n + P$. By employing the forward-backward averaging to effectively double the amount of available data and enhance the detection performance [61], from (4), we define an $M \times 2M$ combined matrix $\overline{\boldsymbol{R}}_{yx}$ as

$$\begin{aligned}\overline{\boldsymbol{R}}_{yx} &\triangleq \left[\boldsymbol{R}_{yx}, \boldsymbol{J}_M\boldsymbol{R}_{yx}^*\right] \\ &= \left[\boldsymbol{A}\Gamma\boldsymbol{R}_{\bar{s}}\Gamma^H\boldsymbol{D}^H\boldsymbol{A}^H, \boldsymbol{A}\overline{\boldsymbol{D}}^{-(M-1)}\Gamma^*\boldsymbol{R}_{\bar{s}}^*\Gamma^T\boldsymbol{D}\boldsymbol{A}^T\right] \\ &= \boldsymbol{A}\boldsymbol{C}\boldsymbol{B}\end{aligned} \tag{6}$$

where

$$\boldsymbol{C} \triangleq \left[\Gamma, \overline{\boldsymbol{D}}^{-(M-1)}\Gamma^*\right], \overline{\boldsymbol{D}} \triangleq \text{blkdiag}\left(\overline{\boldsymbol{D}}_n, \overline{\boldsymbol{D}}_c\right),$$
$$\overline{\boldsymbol{D}}_n \triangleq \text{diag}(e^{j\tau(\alpha_1)}, e^{j\tau(\alpha_2)}, \ldots, e^{j\tau(\alpha_{K_n})}),$$
$$\overline{\boldsymbol{D}}_c \triangleq \text{blkdiag}(\overline{\boldsymbol{D}}_1, \overline{\boldsymbol{D}}_2, , \ldots, \overline{\boldsymbol{D}}_P),$$
$$\overline{\boldsymbol{D}}_p \triangleq \text{diag}(e^{j\tau(\alpha_{p,1})}, e^{j\tau(\alpha_{p,2})}, \ldots, e^{j\tau(\alpha_{p,K_p})}),$$

and $\boldsymbol{B} \triangleq \text{blkdiag}\left(\boldsymbol{R}_{\overline{s}}\Gamma^H\boldsymbol{D}^H\boldsymbol{A}^H, \boldsymbol{R}^*_{\overline{s}}\Gamma^T\boldsymbol{D}\boldsymbol{A}^T\right)$. Evidently $M > K_n + P$, the rank of the $2(K_n+P)\times 2M$ block diagonal matrix $\boldsymbol{B}$ is given by $\rho(\boldsymbol{B}) = 2\rho\left(\boldsymbol{R}_{\overline{s}}\Gamma^H\boldsymbol{D}^H\boldsymbol{A}^H\right) = 2(K_n+P)$. Because the rank of a matrix is not changed by the elementary column operations, the rank of the $K\times 2(K_n+P)$ matrix $\boldsymbol{C}$ is obtained as

$$\begin{aligned}\rho(\boldsymbol{C}) &= \rho\left(\left[\text{blkdiag}\left(\boldsymbol{I}_{K_n}, \Lambda\right),\right.\right.\\ &\qquad \left.\left.\text{blkdiag}\left(\overline{\boldsymbol{D}}_n^{-(M-1)}, \overline{\boldsymbol{D}}_c^{-(M-1)}\Lambda^*\right)\right]\right)\\ &= \rho\left(\text{blkdiag}\left(\left[\boldsymbol{I}_{K_n}, \overline{\boldsymbol{D}}_n^{-(M-1)}\right], \left[\Lambda, \overline{\boldsymbol{D}}_c^{-(M-1)}\Lambda^*\right]\right)\right)\\ &= \rho\left(\left[\boldsymbol{I}_{K_n}, \overline{\boldsymbol{D}}_n^{-(M-1)}\right]\right) + \rho\left(\left[\Lambda, \overline{\boldsymbol{D}}_c^{-(M-1)}\Lambda^*\right]\right) \quad (7)\end{aligned}$$

where

$$\begin{aligned}&\rho\left(\left[\Lambda, \overline{\boldsymbol{D}}_c^{-(M-1)}\Lambda^*\right]\right)\\ &= \rho\left(\text{blkdiag}\left(\left[\boldsymbol{\eta}_1, \overline{\boldsymbol{D}}_1^{-(M-1)}\boldsymbol{\eta}_1^*\right], \ldots, \left[\boldsymbol{\eta}_P, \overline{\boldsymbol{D}}_P^{-(M-1)}\boldsymbol{\eta}_P^*\right]\right)\right)\\ &= \sum_{p=1}^{P}\rho\left(\left[\boldsymbol{\eta}_p, \overline{\boldsymbol{D}}_p^{-(M-1)}\boldsymbol{\eta}_p^*\right]\right) = 2P \quad (8)\end{aligned}$$

and

$$\rho\left(\left[\boldsymbol{I}_{K_n}, \overline{\boldsymbol{D}}_n^{-(M-1)}\right]\right) = K_n.$$

Hence we have the ranks of $\boldsymbol{C}$ and $\overline{\boldsymbol{R}}_{yx}$ as $\rho(\boldsymbol{C}) = K_n + 2P$ and $\rho\left(\overline{\boldsymbol{R}}_{yx}\right) = \min\{K, K_n+2P, 2(K_n+P), M\} = K_n + 2P$ if $M > K$ (i.e., $M > K_n + K_c \geq K_n + 2P$). Then by defining an auto-product matrix $\overline{\Psi}$ of $\overline{\boldsymbol{R}}_{yx}$ in (6) as

$$\overline{\Psi} \triangleq \overline{\boldsymbol{R}}_{yx}\overline{\boldsymbol{R}}^H_{yx} = \boldsymbol{A}\boldsymbol{C}\boldsymbol{B}\boldsymbol{B}^H\boldsymbol{C}^H\boldsymbol{A}^H \quad (9)$$

we easily get $\rho\left(\overline{\Psi}\right) = \rho\left(\overline{\boldsymbol{R}}_{yx}\right) = K_n + 2P$ if $M > K_n + 2P$.

Thus we obtain the relation between the number of noncoherent signals and the ranks of the matrices Ψ and $\overline{\Psi}$ in (5) and (9) as $K_n = 2\rho(\Psi) - \rho\left(\overline{\Psi}\right)$. Then by exploiting the idea proposed in the method for estimating the number of signals without eigendecomposition (MENSE) [30], the ranks of Ψ and $\overline{\Psi}$ can be determined by the QRRC (see Appendix for details), and when the number of snapshots is finite, the number of noncoherent signals can be estimated as

$$\begin{aligned}\hat{K}_n = 2&\left\{\underset{i\in\{1,2,\ldots,M-1\}}{\arg\max}\ \text{QRRC}_{\hat{\Psi}}(i)\right\}\\ &- \underset{i\in\{1,2,\ldots,M-1\}}{\arg\max}\ \text{QRRC}_{\hat{\overline{\Psi}}}(i). \quad (10)\end{aligned}$$

As a result, we can immediately determine the number of the groups of coherent signals (i.e., the coherent sources) as

$$\hat{P} = \underset{i\in\{1,2,\ldots,M-1\}}{\arg\max}\ \text{QRRC}_{\hat{\Psi}}(i) - \hat{K}_n. \quad (11)$$

Remark 2: Theoretically the columns $\boldsymbol{\eta}_p$ and $\overline{\boldsymbol{D}}_p^{-(M-1)}\boldsymbol{\eta}_p^*$ can be linearly correlated with each other in a special case, i.e., $\overline{\boldsymbol{D}}_p^{-(M-1)}\boldsymbol{\eta}_p^* = \text{diag}\left(\varepsilon_{p,1}, \varepsilon_{p,2}, \ldots, \varepsilon_{p,K_p}\right)\boldsymbol{\eta}_p = c\boldsymbol{\eta}_p$ with the equality condition $\varepsilon_{p,1} = \varepsilon_{p,2} = \cdots = \varepsilon_{p,K_p} = c$, where $\varepsilon_{p,k} = e^{-j(M-1)\tau(\alpha_{p,k})}\eta^*_{p,k}/\eta_{p,k}$, and c is a constant factor, and hence the rank of this $K_p\times 2$ matrix $[\boldsymbol{\eta}_p, \overline{\boldsymbol{D}}_p^{-(M-1)}\boldsymbol{\eta}_p^*]$ in (8) is given by $\rho([\boldsymbol{\eta}_p, \overline{\boldsymbol{D}}_p^{-(M-1)}\boldsymbol{\eta}_p^*]) = 1 \neq 2$. However, as studied in the forward/backward spatial smoothing (p. 11, [43]), this case almost never occurs in practice, because the element $\eta_{p,k}$ of $\boldsymbol{\eta}_p$ is a signal property, which represents the complex attenuation of the kth signal $s_{p,k}(t)$ in the pth group with respect to the source signal $s_{cp}(t)$ with $\eta_{p,k} \neq 0$ and $\eta_{p,1} = 1$, and $e^{-j(M-1)\tau(\alpha_{p,k})}\eta^*_{p,k}$ is mainly an array geometry property, which is a function of the intere-sensor phase delay $\tau(\alpha_{p,k})$ in the elevation angle $\alpha_{p,k}$ of kth signal in the pth group with respect to the reference sensor. Thus all $\{\varepsilon_{p,k}\}$ for $k = 1, 2, \ldots, K_P$ will be distinct in an actual situation and the simultaneous equality condition for all $\{\varepsilon_{p,k}\}$ makes it an almost never occurring event. Therefore we can conclude that $\rho([\boldsymbol{\eta}_p, \overline{\boldsymbol{D}}_p^{-(M-1)}\boldsymbol{\eta}_p^*]) = 2$ with probability one (w.p.1). □

B. Oblique Projector with Estimated Elevation Angles of Noncoherent Signals [16]

From (3), we can see that the range spaces $\mathcal{R}(\boldsymbol{A}_n)$ and $\mathcal{R}\left(\overline{\boldsymbol{A}}_c\right)$ associated with the noncoherent and coherent signals are nonoverlapping (or disjoint) and not orthogonal, i.e., $\mathcal{R}\left(\overline{\boldsymbol{A}}\right) = \mathcal{R}(\boldsymbol{A}_n) \oplus \mathcal{R}\left(\overline{\boldsymbol{A}}_c\right)$ and $\mathcal{R}(\boldsymbol{A}_n) \cap \mathcal{R}\left(\overline{\boldsymbol{A}}_c\right) = \{\boldsymbol{0}\}$, where the orthogonal projector does not completely cancel the influence of the noncoherent signals on the detection of the coherent ones. In order to isolate the coherent signals from the noncoherent ones, as studied in [16], we consider the computation of oblique projector without eigendecomposition by using the estimated elevation angles of noncoherent signals obtained from the noisy array data.

By dividing the ULA $\boldsymbol{y}(t)$ into two nonoverlapping forward subarrays with $K_n + P$ and $M - K_n - P$ sensors, the corresponding signal vectors $\overline{\boldsymbol{y}}_1(t)$ and $\overline{\boldsymbol{y}}_2(t)$ is given by

$$\begin{aligned}\overline{\boldsymbol{y}}_1(t) &\triangleq [y_1(t), y_2(t), \ldots, y_{K_n+P}(t)]^T\\ &= \boldsymbol{A}_1\Gamma\overline{\boldsymbol{s}}(t) + \boldsymbol{w}_{\overline{y}_1}(t) \quad (12)\end{aligned}$$

$$\begin{aligned}\overline{\boldsymbol{y}}_2(t) &\triangleq [y_{K_n+P+1}(t), y_{K_n+P+2}(t), \ldots, y_M(t)]^T\\ &= \boldsymbol{A}_2\Gamma\overline{\boldsymbol{s}}(t) + \boldsymbol{w}_{\overline{y}_2}(t) \quad (13)\end{aligned}$$

where $\boldsymbol{A}_1$ and $\boldsymbol{A}_2$ are the submatrices of the $M\times K$ matrix $\boldsymbol{A}$ consisting of the first $K_n + P$ rows or the last $M - K_n - P$ rows, while $\boldsymbol{w}_{\overline{y}_1}(t)$ and $\boldsymbol{w}_{\overline{y}_2}(t)$ are the corresponding vectors of additive noises. From (4), we easily obtain two cross-correlation matrices between $\overline{\boldsymbol{y}}_1(t)$ and $\overline{\boldsymbol{y}}_2(t)$ of these subarrays and $\boldsymbol{x}(t)$ of another ULA as

$$\boldsymbol{R}_{\overline{y}_1 x} \triangleq E\left\{\overline{\boldsymbol{y}}_1(t)\boldsymbol{x}^H(t)\right\} = \overline{\boldsymbol{A}}_1\boldsymbol{R}_{\overline{s}}\Gamma^H\boldsymbol{D}^H\boldsymbol{A}^H \quad (14)$$

$$\boldsymbol{R}_{\overline{y}_2 x} \triangleq E\left\{\overline{\boldsymbol{y}}_2(t)\boldsymbol{x}^H(t)\right\} = \overline{\boldsymbol{A}}_2\boldsymbol{R}_{\overline{s}}\Gamma^H\boldsymbol{D}^H\boldsymbol{A}^H \quad (15)$$

where $\overline{\boldsymbol{A}}_1 \triangleq \boldsymbol{A}_1\Gamma$, and $\overline{\boldsymbol{A}}_2 \triangleq \boldsymbol{A}_2\Gamma$, which are two submatrices of the $M \times (K_n + P)$ matrix $\overline{\boldsymbol{A}}$ given by $\overline{\boldsymbol{A}} = [\overline{\boldsymbol{A}}_1^T, \overline{\boldsymbol{A}}_2^T]^T$. As analyzed early, the generalized array response matrix $\overline{\boldsymbol{A}}$ has a full rank as $\rho(\overline{\boldsymbol{A}}) = K_n + P$, and $\overline{\boldsymbol{A}}_1$ is invertible. Then the rows of $\overline{\boldsymbol{A}}_2$ can be expressed as a linear combination of linearly independent rows of $\overline{\boldsymbol{A}}_1$; equivalently, there is a $(K_n + P) \times (M - K_n - P)$ linear operator $\boldsymbol{P}_{\alpha n}$ between $\overline{\boldsymbol{A}}_2$ and $\overline{\boldsymbol{A}}_1$ [9], [8]

$$\boldsymbol{P}_{\alpha n}^H \overline{\boldsymbol{A}}_1 = \overline{\boldsymbol{A}}_2. \tag{16}$$

From (14) and (15), $\boldsymbol{P}_{\alpha n}$ in (16) can be obtained [9]

$$\boldsymbol{P}_{\alpha n} = \left(\overline{\boldsymbol{A}}_1\right)^{-H} \overline{\boldsymbol{A}}_2^{-H} = \left(\boldsymbol{R}_{\overline{y}_1 x} \boldsymbol{R}_{\overline{y}_1 x}^H\right)^{-1} \boldsymbol{R}_{\overline{y}_1 x} \boldsymbol{R}_{\overline{y}_2 x}^H. \tag{17}$$

Further from (16), we easily get

$$\boldsymbol{Q}_{\alpha n}^H \overline{\boldsymbol{A}} = \boldsymbol{O}_{(M-K_n-P)\times(K_n+P)} \tag{18}$$

where $\boldsymbol{Q}_{\alpha n} \triangleq [\boldsymbol{P}_{\alpha n}^T, -\boldsymbol{I}_{M-K_n-P}^T]^T$. Evidently the columns of the $M \times (M - K_n - P)$ matrix $\boldsymbol{Q}_{\alpha n}$ form a basis of the null space $\mathcal{N}(\overline{\boldsymbol{A}}^H)$ of $\overline{\boldsymbol{A}}^H$, and the orthogonal projector onto $\mathcal{N}(\overline{\boldsymbol{A}}^H)$ is given by $\Pi_{\alpha n} \triangleq \boldsymbol{Q}_{\alpha n}(\boldsymbol{Q}_{\alpha n}^H \boldsymbol{Q}_{\alpha n})^{-1} \boldsymbol{Q}_{\alpha n}^H$, which implies that (e.g., [9], [8])

$$\Pi_{\alpha n} \overline{\boldsymbol{A}} = \boldsymbol{O}_{M\times(K_n+P)}. \tag{19}$$

Since no linear combination of array response vectors with Vandermonde form can result in another array response vectors [43], and in view of $\overline{\boldsymbol{A}} = [\boldsymbol{A}_n, \boldsymbol{A}_c\Lambda]$, where $\boldsymbol{A}_c\Lambda = [\boldsymbol{A}_{c1}\boldsymbol{\eta}_1, \boldsymbol{A}_{c2}\boldsymbol{\eta}_2, \ldots, \boldsymbol{A}_{cP}\boldsymbol{\eta}_P]$, we find that the generalized array response vector $\{\boldsymbol{A}_{cp}\boldsymbol{\eta}_p\}$ for each coherent source is no longer a legitimate array response vector and it does not belong to the array manifold $\boldsymbol{A}$ [10], i.e., $\mathcal{R}(\overline{\boldsymbol{A}}) = \mathcal{R}(\boldsymbol{A}_n) \oplus \mathcal{R}(\boldsymbol{A}_c\Lambda)$ and $\mathcal{R}(\boldsymbol{A}_n) \cap \mathcal{R}(\boldsymbol{A}_c\Lambda) = \{\boldsymbol{0}\}$. Hence it follows that

$$\Pi_{\alpha n} \boldsymbol{A}_n = \boldsymbol{O}_{M\times K_n} \tag{20}$$

$$\Pi_{\alpha n} \boldsymbol{A}_c\Lambda = \boldsymbol{O}_{M\times P}. \tag{21}$$

Thus according to the relation (20), when only finite snapshots of array data are available, the elevation angles $\{\alpha_k\}_{k=1}^{K_n}$ of noncoherent signals can be obtained as the minimizing argument of the following cost function

$$f_n(\alpha) \triangleq \boldsymbol{a}^H(\alpha) \widehat{\Pi}_{\alpha n} \boldsymbol{a}(\alpha) \tag{22}$$

where $\boldsymbol{a}(\alpha) \triangleq \left[1, e^{j\tau(\alpha)}, \ldots, e^{j(M-1)\tau(\alpha)}\right]^T$, and $\tau(\alpha) \triangleq 2\pi d_y \cos\alpha/\lambda$.

Then by defining the orthogonal projector onto the null space $\mathcal{N}(\boldsymbol{A}_n^H)$ of $\boldsymbol{A}_n^H$ as $\Pi_{\mathcal{A}_n}^{\perp} \triangleq \boldsymbol{I}_M - \boldsymbol{A}_n(\boldsymbol{A}_n^H \boldsymbol{A}_n)^{-1} \boldsymbol{A}_n^H$, from (4), we obtain a new $M \times M$ matrix $\tilde{\boldsymbol{R}}_{yx}$ as

$$\tilde{\boldsymbol{R}}_{yx} \triangleq \boldsymbol{R}_{yx} \Pi_{\mathcal{A}_n}^{\perp} = \overline{\boldsymbol{A}}_c \boldsymbol{R}_{\overline{c}} \Lambda^H \boldsymbol{D}_c^H \boldsymbol{A}_c^H \Pi_{\mathcal{A}_n}^{\perp} \tag{23}$$

where $\boldsymbol{D}_c \triangleq \mathrm{diag}(e^{j\gamma(\beta_{1,1})}, e^{j\gamma(\beta_{1,2})}, \ldots, e^{j\gamma(\beta_{P,K_P})})$. Since the rank of $\tilde{\boldsymbol{R}}_{yx}$ is given by $\rho(\tilde{\boldsymbol{R}}_{yx}) = P$, its QR decomposition can be expressed (cf. [45])

$$\begin{aligned}\tilde{\boldsymbol{R}}_{yx}\widetilde{\Pi} = \tilde{\boldsymbol{Q}}\tilde{\boldsymbol{R}} &= [\tilde{\boldsymbol{q}}_1, \tilde{q}_2, \ldots, \tilde{\boldsymbol{q}}_M] \begin{bmatrix} \tilde{\boldsymbol{R}}_1 \\ \boldsymbol{O}_{(M-P)\times M} \end{bmatrix} \begin{matrix} \}P \\ \}M-P \end{matrix} \\ &= \tilde{\boldsymbol{Q}}_1 \tilde{\boldsymbol{R}}_1 \end{aligned} \tag{24}$$

where $\tilde{\boldsymbol{Q}}$ is the $M \times M$ unitary matrix given by $\tilde{\boldsymbol{Q}} \triangleq [\tilde{\boldsymbol{Q}}_1, \tilde{\boldsymbol{Q}}_2]$ with $\tilde{\boldsymbol{Q}}_1 \triangleq [\tilde{\boldsymbol{q}}_1, \tilde{\boldsymbol{q}}_2, \ldots, \tilde{\boldsymbol{q}}_P], \tilde{\boldsymbol{Q}}_2 \triangleq [\tilde{\boldsymbol{q}}_{P+1}, \tilde{\boldsymbol{q}}_{P+2}, \ldots, \tilde{\boldsymbol{q}}_M]$, and $\tilde{\boldsymbol{R}}_1$ is a $P \times M$ full row rank matrix, while $\widetilde{\Pi}$ is the $M \times M$ permutation matrix, which does not change the correlation of the columns in $\tilde{\boldsymbol{R}}_{yx}$. From (23) and (24), we can see that $\mathcal{R}(\tilde{\boldsymbol{R}}_{yx}) = \mathcal{R}(\overline{\boldsymbol{A}}_c) = \mathcal{R}(\tilde{\boldsymbol{Q}}_1)$ and the orthogonal projector onto $\mathcal{N}(\tilde{\boldsymbol{Q}}_1^H)$ can be obtained

$$\Pi_{\tilde{\mathcal{Q}}_1}^{\perp} \triangleq \boldsymbol{I}_M - \tilde{\boldsymbol{Q}}_1(\tilde{\boldsymbol{Q}}_1^H \tilde{\boldsymbol{Q}}_1)^{-1} \tilde{\boldsymbol{Q}}_1^H = \tilde{\boldsymbol{Q}}_2 \tilde{\boldsymbol{Q}}_2^H. \tag{25}$$

Consequently by using the property that orthogonal projector is invariant to change of the base, we have the orthogonal projector onto $\mathcal{N}(\overline{\boldsymbol{A}}_c^H)$ defined by $\Pi_{\overline{\mathcal{A}}_c}^{\perp} \triangleq \boldsymbol{I}_M - \overline{\boldsymbol{A}}_c(\overline{\boldsymbol{A}}_c^H \overline{\boldsymbol{A}}_c)^{-1} \overline{\boldsymbol{A}}_c^H$ as (see (Appendix A, [16]) for details)

$$\Pi_{\overline{\mathcal{A}}_c}^{\perp} = \Pi_{\tilde{\mathcal{Q}}_1}^{\perp} = \tilde{\boldsymbol{Q}}_2 \tilde{\boldsymbol{Q}}_2^H. \tag{26}$$

Hence by expressing the oblique projector which projects onto the space $\mathcal{R}(\boldsymbol{A}_n)$ along a direction parallel to the space $\mathcal{R}(\overline{\boldsymbol{A}}_c)$ as $\boldsymbol{E}_{\mathcal{A}_n|\overline{\mathcal{A}}_c}$, which is given by (e.g., [60])

$$\boldsymbol{E}_{\mathcal{A}_n|\overline{\mathcal{A}}_c} \triangleq \boldsymbol{A}_n \left(\boldsymbol{A}_n^H \Pi_{\overline{\mathcal{A}}_c}^{\perp} \boldsymbol{A}_n\right)^{-1} \boldsymbol{A}_n^H \Pi_{\overline{\mathcal{A}}_c}^{\perp} \tag{27}$$

where $\boldsymbol{E}_{\mathcal{A}_n|\overline{\mathcal{A}}_c} \boldsymbol{A}_n = \boldsymbol{A}_n$, and $\boldsymbol{E}_{\mathcal{A}_n|\overline{\mathcal{A}}_c} \overline{\boldsymbol{A}}_c = \boldsymbol{O}_{M\times P}$. From (26) and (27), we can obtain the oblique projector $\boldsymbol{E}_{\mathcal{A}_n|\overline{\mathcal{A}}_c}$ as

$$\boldsymbol{E}_{\mathcal{A}_n|\overline{\mathcal{A}}_c} = \boldsymbol{A}_n \left(\boldsymbol{A}_n^H \tilde{\boldsymbol{Q}}_2 \tilde{\boldsymbol{Q}}_2^H \boldsymbol{A}_n\right)^{-1} \boldsymbol{A}_n^H \tilde{\boldsymbol{Q}}_2 \tilde{\boldsymbol{Q}}_2^H. \tag{28}$$

Evidently the oblique projector $\boldsymbol{E}_{\mathcal{A}_n|\overline{\mathcal{A}}_c}$ in (28) is not affected by the unknown projector $\Pi_{\overline{\mathcal{A}}_c}^{\perp}$ and can be obtained from $\boldsymbol{R}_{yx}$ and $\boldsymbol{A}_n$ (i.e., the elevation angles $\{\alpha_k\}_{k=1}^{K_n}$ of the noncoherent signals) with available array data, while the eigendecomposition is not required.

C. Determination of Source Coherency Structure

Now we consider the determination of the numbers of coherent signals in each group (i.e., the source coherency structure) by utilizing the oblique projector $\boldsymbol{E}_{\mathcal{A}_n|\overline{\mathcal{A}}_c}$ obtained in (28) to isolate the coherent signals from the noncoherent ones and by applying the forward subarray averaging to decorrelate the coherency of some incident signals.

By using the properties of oblique projector, from (28) and (3), we obtain the projected data vector $\tilde{\boldsymbol{y}}(t)$ as

$$\begin{aligned}\tilde{\boldsymbol{y}}(t) &\triangleq \left(\boldsymbol{I}_M - \boldsymbol{E}_{\mathcal{A}_n|\overline{\mathcal{A}}_c}\right) \boldsymbol{y}(t) \\ &= \boldsymbol{A}_c\Lambda\overline{\boldsymbol{s}}_c(t) + \left(\boldsymbol{I}_M - \boldsymbol{E}_{\mathcal{A}_n|\overline{\mathcal{A}}_c}\right) \boldsymbol{w}_y(t). \end{aligned} \tag{29}$$

Clearly the noncoherent signals are eliminated in (29). From (2) and (29), we obtain a new cross-correlation matrix $\boldsymbol{R}_{\tilde{y}x}$ as

$$\boldsymbol{R}_{\tilde{y}x} \triangleq E\{\tilde{\boldsymbol{y}}(t)\boldsymbol{x}^H(t)\} = \left(\boldsymbol{I}_M - \boldsymbol{E}_{\mathcal{A}_n|\overline{\mathcal{A}}_c}\right) \boldsymbol{R}_{yx} \tag{30}$$

$$= \boldsymbol{A}_c\Lambda\boldsymbol{R}_{\overline{c}}\Lambda^H \boldsymbol{D}_c^H \boldsymbol{A}_c^H \tag{31}$$

where $\boldsymbol{R}_{\tilde{y}x}$ only contains the information of coherent signals. In the following, we deal with the number detection of coherent signals in each group (i.e., $\{K_p\}_{p=1}^P$) from $\boldsymbol{R}_{\tilde{y}x}$.

By defining the $(M-m)\times M$ selection matrix $\boldsymbol{F}_m^{(r)}$ as

$$\boldsymbol{F}_m^{(r)} \triangleq \left[\boldsymbol{O}_{(M-m)\times(r-1)}, \boldsymbol{I}_{M-m}, \boldsymbol{O}_{(M-m)\times(m-r+1)}\right] \quad (32)$$

where $r=1,2,\ldots,m+1$, and $0\le m\le \overline{M}\le M-K_c-1$ (see Remark 3 for the determination of $\overline{M}$), we obtain a telescoping series of the matrix $\boldsymbol{R}_{\tilde{y}x}$ as (cf. [39])

$$\{\boldsymbol{T}_0, \boldsymbol{T}_1, \boldsymbol{T}_2, \ldots, \boldsymbol{T}_{\overline{M}}\} \quad (33)$$

where the $(M-m)\times M(m+1)$ telescoping matrix $\boldsymbol{T}_m$ is defined by

$$\boldsymbol{T}_m \triangleq \left[\boldsymbol{T}_m^{(1)}, \boldsymbol{T}_m^{(2)}, \ldots, \boldsymbol{T}_m^{(m+1)}\right] \quad (34)$$

in which the rth $(M-m)\times M$ submatrix $\boldsymbol{T}_m^{(r)}$ is given by

$$\boldsymbol{T}_m^{(r)} \triangleq \boldsymbol{F}_m^{(r)}\boldsymbol{R}_{\tilde{y}x} \quad (35)$$

$$= \boldsymbol{A}_c^{(m)}\overline{\boldsymbol{D}}_c^{r-1}\Lambda\boldsymbol{R}_{\bar{c}}\Lambda^H\boldsymbol{D}_c^H\boldsymbol{A}_c^H \quad (36)$$

and $\boldsymbol{A}_c^{(m)}$ is the submatrix of $\boldsymbol{A}_c$ consisting of the first $M-m$ rows, while evidently $\boldsymbol{T}_0=\boldsymbol{R}_{\tilde{y}x}$. By substituting (36) into (34), we can reexpress $\boldsymbol{T}_m$ as

$$\boldsymbol{T}_m = \boldsymbol{A}_c^{(m)}\boldsymbol{C}_m\boldsymbol{G}_m \quad (37)$$

where the $K_c\times(m+1)P$ matrix $\boldsymbol{C}_m$ and the $(m+1)P\times(m+1)M$ matrix $\boldsymbol{G}_m$ are given by

$$\boldsymbol{C}_m \triangleq \left[\Lambda, \overline{\boldsymbol{D}}_c\Lambda, \ldots, \overline{\boldsymbol{D}}_c^m\Lambda\right] \quad (38)$$

$$\boldsymbol{G}_m \triangleq \boldsymbol{I}_{m+1}\otimes\left(\boldsymbol{R}_{\bar{c}}\Lambda^H\boldsymbol{D}_c^H\boldsymbol{A}_c^H\right) \quad (39)$$

and $\boldsymbol{A}_c^{(m)}$ is full column rank with $\rho\left(\boldsymbol{A}_c^{(m)}\right)=K_c$ if $M-m\ge K_c$, while the $\boldsymbol{G}_m$ is full row rank with

$$\rho(\boldsymbol{G}_m)=\rho(\boldsymbol{I}_{m+1})\,\rho\left(\boldsymbol{R}_{\bar{c}}\Lambda^H\boldsymbol{D}_c^H\boldsymbol{A}_c^H\right)=(m+1)P. \quad (40)$$

Hence we obtain the rank of the telescoping matrix $\boldsymbol{T}_m$ as

$$\rho(\boldsymbol{T}_m)=\rho(\boldsymbol{C}_m). \quad (41)$$

Further since the rank of a matrix is not changed by the elementary column operations, the rank of $\boldsymbol{C}_m$ is obtain

$$\begin{aligned}\rho(\boldsymbol{C}_m) &= \rho(\mathrm{blkdiag}(\boldsymbol{\eta}_1,\ldots,\boldsymbol{\eta}_P), \mathrm{blkdiag}\Big(\overline{\boldsymbol{D}}_1\boldsymbol{\eta}_1,\ldots,\\ &\quad \overline{\boldsymbol{D}}_P\boldsymbol{\eta}_P\Big),\ldots,\mathrm{blkdiag}\Big(\overline{\boldsymbol{D}}_1^m\boldsymbol{\eta}_1,\ldots,\overline{\boldsymbol{D}}_P^m\boldsymbol{\eta}_P\Big)\Big)\\ &= \sum_{p=1}^{P}\rho\Big(\Big[\boldsymbol{\eta}_p,\overline{\boldsymbol{D}}_p\boldsymbol{\eta}_p,\ldots,\overline{\boldsymbol{D}}_p^m\boldsymbol{\eta}_p\Big]\Big)\\ &= \sum_{p=1}^{P}\rho\left(\overline{\boldsymbol{H}}_p(\tilde{\boldsymbol{A}}_{cp}^{(m)})^T\right)\end{aligned} \quad (42)$$

where $\overline{\boldsymbol{H}}_p \triangleq \mathrm{diag}(\eta_{p,1},\eta_{p,2},\ldots,\eta_{p,K_p})$, and $\tilde{\boldsymbol{A}}_{cp}^{(m)}$ is a submatrix of $\boldsymbol{A}_{cp}$ consisting of the first $m+1$ rows. Evidently $\overline{\boldsymbol{H}}_p$ is full rank matrix, and the rank of $\tilde{\boldsymbol{A}}_{cp}^{(m)}$ is given by $\rho(\tilde{\boldsymbol{A}}_{cp}^{(m)})=\min\{m+1,K_p\}$. Then from (42), we have

$$\rho(\boldsymbol{C}_m)=\sum_{p=1}^{P}\min\{m+1,K_p\}. \quad (43)$$

Thus when $M-m\ge K_c$, from (41) and (43), we obtain the rank of telescoping matrix $\boldsymbol{T}_m$ in (37) (i.e., (34)) as

$$\rho(\boldsymbol{T}_m)=\rho(\boldsymbol{C}_m)=\sum_{p=1}^{P}\min\{m+1,K_p\}. \quad (44)$$

Then by denoting the number of coherent groups with degree l as $\{g_l\}$ for $l=2,3,\ldots,L$ (cf. [39]), i.e., g_l denotes the number of groups with l coherent signals, we have the relations between the number of coherent groups P, the numbers of coherent signals in each group $\{K_p\}$, and the total number of coherent signals K_c as

$$\sum_{l=2}^{L}g_l=P, \sum_{l=2}^{L}lg_l=\sum_{p=1}^{P}K_p=K_c. \quad (45)$$

Clearly we note that $\{g_2,g_3,\ldots,g_L\}$ and $\{K_1,K_2,\ldots,K_P\}$ are equivalent characterization of the source coherency structure, and hence the determination of numbers of coherent signals $\{K_p\}$ is converted to the estimation of $\{g_2,g_3,\ldots,g_L\}$. From (44) and (45), the rank of $\boldsymbol{T}_m$ can be expressed as

$$\rho(\boldsymbol{T}_m)=\begin{cases}P, & m=0\\ \sum_{l=2}^{m+1}lg_l+(m+1)\sum_{l=m+2}^{L}g_l, & 1\le m\le L-2\\ K_c, & m\ge L-1\end{cases} \quad (46)$$

and from (46), we can get

$$\rho(\boldsymbol{T}_{m+1})-\rho(\boldsymbol{T}_m)=\sum_{l=m+2}^{L}g_l>0 \quad (47)$$

for $0\le m\le L-2$. Further by defining the outer-product matrix Φ_m of $\boldsymbol{T}_m$ in (37) (i.e., (34)) as

$$\Phi_m \triangleq \boldsymbol{T}_m\boldsymbol{T}_m^H \quad (48)$$

we easily obtain the rank of this $(M-m)\times(M-m)$ matrix Φ_m as $\rho(\Phi_m)=\rho(\boldsymbol{T}_m)$. From (46) and (47), we find that the rank of Φ_m increases monotonously until it reaches K_c with the increasing m, while it and the number of coherent groups $\{g_l\}$ satisfy the relation as

$$g_{m+2}=2\rho(\Phi_{m+1})-\rho(\Phi_m)-\rho(\Phi_{m+2}) \quad (49)$$

for $0\le m\le L-2$, and the rank of the telescoping matrix Φ_m becomes to be stationary as (cf. [39], [27])

$$\rho(\Phi_{L-1})=\rho(\Phi_L)=\cdots=\rho(\Phi_{M-K_c-1})=K_c \quad (50)$$

for $L-1\le m\le M-K_c-1$.

Thus from (49) and (50), when only finite snapshots of array data are available, the numbers of coherent groups $\{g_l\}$ with degree l and the number of coherent signals K_c can be estimated from the ranks of telescoping matrices $\{\widehat{\Phi}_m\}$ (i.e., $\{\hat{\boldsymbol{T}}_m\}$) with

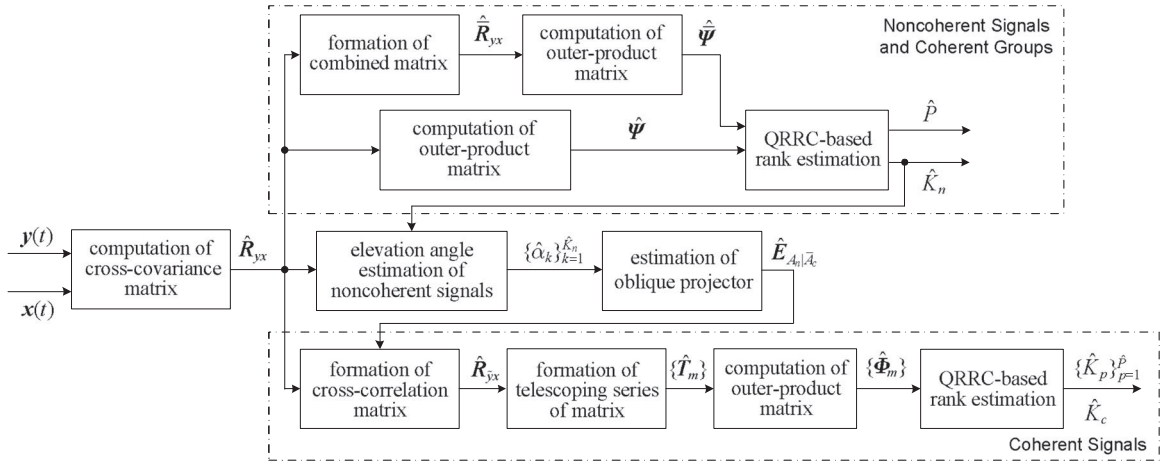

Fig. 2. The simplified flowchart of the proposed OPEMS for estimating the number of noncoherent signals and that of coherent signals with multiple groups.

the QRRC as

$$\rho\left(\widehat{\Phi}_m\right) = \underset{i\in\{1,2,\ldots,M-m-1\}}{\arg\max} \mathrm{QRRC}_{\widehat{\Phi}_m}(i) \tag{51}$$

$$\hat{L} = m, \quad \text{if } \rho\left(\widehat{\Phi}_m\right) = \rho\left(\widehat{\Phi}_{m-1}\right) \text{ and } \rho\left(\widehat{\Phi}_{m-1}\right) > \rho\left(\widehat{\Phi}_{m-2}\right) \tag{52}$$

$$\hat{K}_c = \rho\left(\widehat{\Phi}_{\hat{L}}\right) \tag{53}$$

$$\hat{g}_{m+2} = 2\rho\left(\widehat{\Phi}_{m+1}\right) - \rho\left(\widehat{\Phi}_m\right) - \rho\left(\widehat{\Phi}_{m+2}\right), \quad \text{for } 0 \le m \le \hat{L}-2 \tag{54}$$

and hence we can determine the numbers of coherent signals $\{\hat{K}_p\}_{p=1}^{\hat{P}}$ from $\{\hat{g}_l\}_{l=2}^{\hat{L}}$, which characterize the same coherency structure of incident coherent signals with multiple groups.

Remark 3: Under Assumption 4, the rank profile of the telescoping series of matrices $\{\Phi_m\}$ has two stationary points as $\rho(\Phi_{L-1}) = \rho(\Phi_L) = K_c$, if the number of sensors M equals the minimum number of sensors required by the OPEMS, i.e., $M = M_{\mathrm{OPEMS}} \triangleq \max\{K_n + 2P, K_c + L\} + 1$ (see Remark 6 for details), while it has more than two stationary points as $\rho(\Phi_{L-1}) = \rho(\Phi_L) = \cdots = \rho(\Phi_{M-K_c-1}) = K_c$ if $M > M_{\mathrm{OPEMS}}$. Hence the parameter $\overline{M}$ in (32) can be determined as $\overline{M} = m = L$ if $\rho(\Phi_m) = \rho(\Phi_{m-1})$ for $m = 1, 2, \ldots$. □

D. Implementation of Proposed OPEMS

When finite array data $\{\boldsymbol{y}(t)\}_{t=1}^{N_t}$ and $\{\boldsymbol{x}(t)\}_{t=1}^{N_t}$ are available, as shown in Fig. 2, the implementation of the proposed OPEMS can be summarized as follows.

Step 1: Calculate the sample cross-correlation matrix $\hat{\boldsymbol{R}}_{yx}$ from the array data $\{\boldsymbol{y}(t)\}_{t=1}^{N_t}$ and $\{\boldsymbol{x}(t)\}_{t=1}^{N_t}$ as

$$\hat{\boldsymbol{R}}_{yx} = \frac{1}{N_t}\sum_{t=1}^{N_t} \boldsymbol{y}(t)\,\boldsymbol{x}^H(t). \tag{55}$$

..... $8M^2N_t + 6M^2$ flops

Step 2: By forming the estimates $\widehat{\Psi}$ with (5) and $\widehat{\overline{\Psi}}$ with (6) and (9) from $\hat{\boldsymbol{R}}_{yx}$, estimate the number of noncoherent signals K_n and that of the groups of coherent signals P with (10) and (11). ..... $52M^3 - 7M^2 + 53M$ flops

Step 3: By partitioning the matrix $\hat{\boldsymbol{R}}_{yx}$ as

$$\hat{\boldsymbol{R}}_{yx} = \begin{bmatrix} \hat{\boldsymbol{R}}_{\overline{y}_1 x} \\ \hat{\boldsymbol{R}}_{\overline{y}_2 x} \end{bmatrix} \begin{matrix} \}\hat{K}_n + \hat{P} \\ \}M - (\hat{K}_n + \hat{P}) \end{matrix} \tag{56}$$

calculate the estimated linear operator $\hat{\boldsymbol{P}}_{\alpha n}$ from $\hat{\boldsymbol{R}}_{\overline{y}_1 x}$ and $\hat{\boldsymbol{R}}_{\overline{y}_2 x}$ with (17) and estimate the elevation angles $\{\alpha_k\}_{k=1}^{\hat{K}_n}$ of noncoherent signals with (22) by finding the phases of the $\hat{K}_n$ zeros of the polynomial $p_{\alpha n}(z)$ closest to the unit circle in the z-plane

$$p_{\alpha n}(z) \triangleq z^{M-1}\boldsymbol{p}^H(z)\,\widehat{\Pi}_{\alpha n}\boldsymbol{p}(z) \tag{57}$$

where $z \triangleq e^{j\tau(\alpha)}$, and $\boldsymbol{p}(z) \triangleq \left[1, z, \ldots, z^{M-1}\right]^T$.

$$\ldots 16M^3 - 8M^2\overline{K} + 16M\overline{K}^2 + 2M^2 - 8\overline{K}^3 - 4M\overline{K} + 4\overline{K}^2 + (M-1)^2 + O\left(\overline{K}^3\right) + O\left((2M-1)^2\right) \text{ flops}$$

Step 4: By calculating the estimated oblique projector $\hat{\boldsymbol{E}}_{\mathcal{A}_n|\overline{\mathcal{A}}_c}$ from $\hat{\boldsymbol{R}}_{yx}$ and $\widehat{\Pi}^{\perp}_{\mathcal{A}_n}$ (i.e., $\hat{\boldsymbol{A}}_n$ or $\{\hat{\alpha}_k\}_{k=1}^{\hat{K}_n}$) with (23), (24) and (28), form the estimate $\hat{\boldsymbol{R}}_{\tilde{y}x}$ with (30). .....$38M^3 - 2M^2 + 32MK_n^2 + 24M^2K_n - 8M^2P - 8PK_n^2 - 16MK_nP + 2O\left(K_n^3\right)$ flops

Step 5: By setting $m = 0$, denote $\hat{\boldsymbol{T}}_0$ as $\hat{\boldsymbol{T}}_0 = \hat{\boldsymbol{R}}_{\tilde{y}x}$ and the rank of $\widehat{\Phi}_0$ as $\rho\left(\widehat{\Phi}_0\right) = \hat{P}$. .....0 flops

Step 6: By setting $m = m + 1$ and forming the estimate $\hat{\boldsymbol{T}}_m$ with (32), (34) and (35), estimate the rank of $\widehat{\Phi}_m$ with (51). ..... $8M(M-m)^2(m+1) + 14(M-m)^3 - 6(M-m)^2 + 22(M-m)$ flops

Step 7: If $\rho(\widehat{\Phi}_m) \neq \rho(\widehat{\Phi}_{m-1})$, return to Step 6; otherwise, estimate the highest degree of coherency L and the number of coherent signals K_c with (52) and (53). ..... 0 flops

Step 8: By using the estimated ranks $\{\rho(\widehat{\Phi}_0), (\widehat{\Phi}_1), \ldots, \rho(\widehat{\Phi}_m)\}$, estimate $\{g_l\}_{l=2}^{\hat{L}}$ with (54) and the numbers of coherent signals $\{\hat{K}_p\}_{p=1}^{\hat{P}}$ with $\{\hat{g}_l\}_{l=2}^{\hat{L}}$. ..... $4m$ `flops`

In above, the computational complexity of each step is roughly indicated in terms of the number of MATLAB flops, where a flop is defined as a floating-point addition or multiplication operation, and the estimates $\hat{K}_n$ and $\hat{P}$ are replaced with their true values K_n and P for convenience. Hence the computational complexity of the proposed OPEMS is approximately $8M^2N_t + 106M^3 + (L+1)\left(4LM^3 + 14M^3\right)$ flops when $M \gg K$, which occurs often in applications of array processing.

Remark 4: In Step 3, the orthogonal projector $\widehat{\Pi}_{\alpha n}$ is calculated by using the matrix inversion lemma implicitly [9], and the polynomial roots can be found by using the Lindsey-Fox root finding algorithm [66] (see (Remark 5, [16]) for details). □

Remark 5: The SRP test [39] can be extended to the enumeration problem with two parallel ULAs considered herein, and its implementation consists of the following four major steps: 1) computation of the sample cross-covariance matrix $\hat{\boldsymbol{R}}_{yx}$ as (55), where it requires $8M^2N_t + 6M^2$ flops; 2) formulation of the $m \times m$ spatially smoothed cross-covariance matrix $\widehat{\overline{\boldsymbol{R}}}_m$ from $\hat{\boldsymbol{R}}_{yx}$ as $\widehat{\overline{\boldsymbol{R}}}_m = (1/(M-m+1)) \sum_{l=1}^{M-m+1} \hat{\boldsymbol{R}}_m^{(l)}$ for $1 < m \leq M$, where it needs $2m^2(M-m+1) + 6m^2$ flops for $m \neq M$, $\hat{\boldsymbol{R}}_m^{(l)}$ is the $m \times m$ principal diagonal submatrix of $\hat{\boldsymbol{R}}_{yx}$ given by $\hat{\boldsymbol{R}}_m^{(l)} = \overline{\boldsymbol{F}}_m^{(l)} \hat{\boldsymbol{R}}_{yx} (\overline{\boldsymbol{F}}_m^{(l)})^T$, and $\overline{\boldsymbol{F}}_m^{(l)} \triangleq [\boldsymbol{O}_{m\times(l-1)}, \boldsymbol{I}_m, \boldsymbol{O}_{m\times(M-m-l+1)}]$; 3) eigenvalue decomposition (EVD) of $\widehat{\overline{\boldsymbol{R}}}_m$ for estimation of its eigenvalues $\{\widehat{\overline{\lambda}}_m^{(i)}\}$ for $i = 1, 2, \ldots, m$, where it costs $\mathcal{O}(m^3)$ flops; and 4) calculation of MDL criterion [17] for the rank determination of $\widehat{\overline{\boldsymbol{R}}}_m$ with $\{\widehat{\overline{\lambda}}_m^{(i)}\}$, where it requires $m(m+16)$ flops. Especially the last three steps should be repeated for many times to obtain the set of ranks of the telescoping series $\{\widehat{\overline{\boldsymbol{R}}}_m\}$ (i.e., the SRP of $\hat{\boldsymbol{R}}_{yx}$) (for example, $m = M, M-1, \ldots, M-L$), and hence the estimated number of MATLAB flops required by the SRP test is approximately $8M^2N_t + 6M^2 + \mathcal{O}(M^3) + M(M+16) + \sum_{m=M-L}^{M-1}(\mathcal{O}(m^3) + m(m+16) + 2m^2(M-m+1) + 6m^2)$ flops (cf. (Remark 6, [30])).

By denoting the numbers of MATLAB flops required by the SRP test and the OPEMS as f_{SRP} and f_{OPEMS}, we define the relative efficiency ratio as $f_{\mathrm{OPEMS}}/f_{\mathrm{SRP}}$. With some simulation-based examinations, the relative efficiency ratio $f_{\mathrm{OPEMS}}/f_{\mathrm{SRP}}$ in terms of the number of sensors M of one ULA is shown in Fig. 3(a) for different highest degree of coherency L, where M is verified from $M = 11$ to $M = 90$, L is varied from $L = 2, 3, 4$ to 5, and $N_t = 100$, while the ratio versus the number of snapshots N_t is plotted in Fig. 3(b) for different number of sensors M, where N_t is verified from $N_t = 20$ to $N_t = 5,000$, M is varied from $M = 10, 14$ to 18, and $L = 3$. From Fig. 3, we can find that $f_{\mathrm{OPEMS}}/f_{\mathrm{SRP}} < 1$ (i.e., $f_{\mathrm{OPEMS}} < f_{\mathrm{SRP}}$) and $f_{\mathrm{OPEMS}}/f_{\mathrm{SRP}}$ decreases monotonically with the increasing M, while $f_{\mathrm{OPEMS}}/f_{\mathrm{SRP}}$ increases monotonically with the increasing N_t and approaches 1 when $N_t \gg M$ and $N_t \to \infty$ as the computational complexities of two methods will be dominated by the term $8M^2N_t$ (i.e., the calculation of the sample cross-covariance matrix) in this case. Evidently the computational complexity of the OPEMS is much less than that of the SRP test, and the computational load of the SRP test is mostly dominated by the calculation of the sample cross-covariance matrix and the EVD procedures of the telescoping series of matrices with different dimensions (i.e., Steps 1 and 3), when the number of snapshots N_t is not significantly larger than the number of sensors M. Hence the quantitative comparisons show that the OPEMS is computationally efficient than the SRP test with EVD-based MDL, where the eigendecomposition procedure is avoided in the OPEMS. □

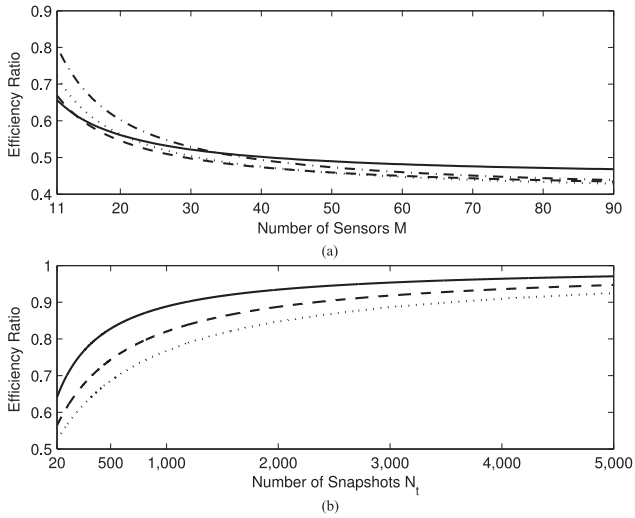

Fig. 3. The relative efficiency ratio between the estimated number of MATLAB flops required by the proposed OPEMS and that of the SRP test in terms of (a) the number of sensors (solid line: $L = 2$; dashed line: $L = 3$; dotted line: $L = 4$; and dash-dotted line: $L = 5$; $N_t = 100$) and (b) the number of snapshots (solid line: $M = 10$; dashed line: $M = 14$; dotted line: $M = 18$; and $L = 3$). (a) Comparison of Computational Complexity versus Number of Sensors. (b) Comparison of Computational Complexity versus Number of Snapshots.

Remark 6: In the proposed OPEMS, the resolvable conditions for estimating the numbers of noncoherent and coherent signals are $M > K_n + 2P$, $M - m > K_c$, and $m \geq L = \max\{K_p\}$. Hence the minimum number of sensors required by the OPEMS is $M_{\mathrm{OPEMS}} = \max\{K_n + 2P, K_c + L\} + 1$, while that necessitated by the SRP test [39] is $M_{\mathrm{SRP}} = K_n + K_c + L + 1$. By considering that the relation $K_c \geq 2P$, we can find that the OPEMS requires less number of sensors than the SRP test for a fixed number of incident signals, i.e., the OPEMS can detect more incident signals with the fixed number of sensors. □

Remark 7: In this paper, the array geometry of two parallel ULAs is exploited to decorrelate the coherency of incident signals with the forward/backward subarray averaging [42], [43], [61], and the cross-correlations between two ULAs are used to alleviate the effect of additive noises. By selecting two arbitrary ULAs parallel to or along the y axis as depicted in Fig. 4, the proposed OPEMS can be straightforwardly extended as an enumerator to the 2-D DOA estimation with a uniform rectangular array (e.g., [2], [13], [67]), which can be regarded as the planar array consisting of more than two parallel ULAs. □

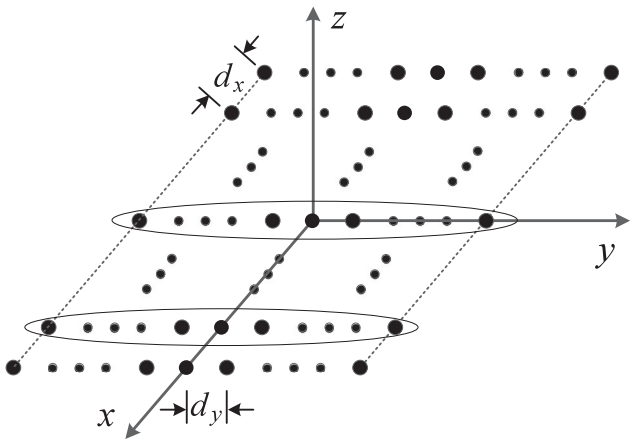

Fig. 4. The extension of the proposed OPEMS to a uniform rectangular planar array.

IV. Consistency of Proposed OPEMS

In this section, we study the consistency property of the proposed OPEMS and show that the OPEMS can yield the correct number of the noncoherent signals and that of the coherent signals in each coherent group w.p.1 as the number of snapshots approaches to infinity. Firstly we consider the asymptotical errors of $\widehat{\Psi}$, $\widehat{\overline{\Psi}}$ and $\widehat{\Phi}_m$.

Theorem 1: The asymptotical errors of the estimates of Ψ, $\overline{\Psi}$ and Φ_m in (5), (9) and (48) are given by

$$E\{\widehat{\Psi}-\Psi\}=\frac{1}{N_t}\mathrm{tr}\left(\boldsymbol{R}_{xx}\right)\boldsymbol{R}_{yy} \tag{58}$$

$$E\{\widehat{\overline{\Psi}}-\overline{\Psi}\}=\frac{1}{N_t}\mathrm{tr}\left(\boldsymbol{R}_{xx}\right)\left(\boldsymbol{R}_{yy}+\boldsymbol{J}_M\boldsymbol{R}_{yy}^{*}\boldsymbol{J}_M\right) \tag{59}$$

$$\begin{aligned}E\{\widehat{\Phi}_m-\Phi_m\}=\frac{1}{N_t}\mathrm{tr}\left(\boldsymbol{R}_{xx}\right)\boldsymbol{F}_m\Big\{\boldsymbol{I}_{m+1}\otimes\Big(\Big(\boldsymbol{I}_M-\boldsymbol{E}_{\mathcal{A}_n|\overline{\mathcal{A}}_c}\Big)\\ \cdot\boldsymbol{R}_{yy}\Big(\boldsymbol{I}_M-\boldsymbol{E}_{\mathcal{A}_n|\overline{\mathcal{A}}_c}\Big)^H\Big)\Big\}\boldsymbol{F}_m^H\end{aligned} \tag{60}$$

where $\boldsymbol{R}_{yy}$ and $\boldsymbol{R}_{xx}$ are the covariance matrices of the received signals $\boldsymbol{y}(t)$ and $\boldsymbol{x}(t)$ in (3) and (2) given by

$$\boldsymbol{R}_{yy}\triangleq E\left\{\boldsymbol{y}(t)\,\boldsymbol{y}^H(t)\right\}=\overline{\boldsymbol{A}}\boldsymbol{R}_{\overline{s}}\overline{\boldsymbol{A}}^H+\sigma^2\boldsymbol{I}_M \tag{61}$$

$$\begin{aligned}\boldsymbol{R}_{xx}&\triangleq E\left\{\boldsymbol{x}(t)\,\boldsymbol{x}^H(t)\right\}\\&=\boldsymbol{A}\boldsymbol{D}\Gamma\boldsymbol{R}_{\overline{s}}\Gamma^H\boldsymbol{D}^H\boldsymbol{A}^H+\sigma^2\boldsymbol{I}_M\end{aligned} \tag{62}$$

and $\boldsymbol{F}_m$ is a matrix constructed by the selection matrices $\{\boldsymbol{F}_m^{(r)}\}_{r=1}^{m+1}$ in (32) defined as

$$\boldsymbol{F}_m\triangleq\left[\boldsymbol{F}_m^{(1)},\boldsymbol{F}_m^{(2)},\ldots,\boldsymbol{F}_m^{(m+1)}\right] \tag{63}$$

for $m=0,1,\ldots,\overline{M}$.

Proof: Under the basic assumptions and with the formula for the expectation of the product of four complex Gaussian random vectors with zero-mean (cf. [68]), from (5) and (55), we have

$$\begin{aligned}E\left\{\widehat{\Psi}\right\}&=E\left\{\hat{\boldsymbol{R}}_{yx}\hat{\boldsymbol{R}}_{yx}^H\right\}\\&=\frac{1}{N_t^2}\sum_{t=1}^{N_t}\sum_{n=1}^{N_t}E\left\{\boldsymbol{y}(t)\,\boldsymbol{x}^H(t)\,\boldsymbol{x}(n)\,\boldsymbol{y}^H(n)\right\}\\&=\frac{1}{N_t^2}\sum_{t=1}^{N_t}\sum_{n=1}^{N_t}\Big(E\left\{\boldsymbol{y}(t)\,\boldsymbol{x}^H(t)\right\}E\left\{\boldsymbol{x}(n)\,\boldsymbol{y}^H(n)\right\}\\&\quad+\sum_{i=1}^{M}E\left\{\left(\boldsymbol{e}_i^T\boldsymbol{x}(n)\right)\otimes\boldsymbol{y}(t)\right\}\\&\quad\cdot E\left\{\boldsymbol{y}^H(n)\otimes\left(\boldsymbol{x}^H(t)\,\boldsymbol{e}_i\right)\right\}\\&\quad+E\left\{\boldsymbol{y}(t)\,E\left\{\boldsymbol{x}^H(t)\,\boldsymbol{x}(n)\right\}\boldsymbol{y}^H(n)\right\}-\boldsymbol{O}_{M\times M}\Big)\\&=\frac{1}{N_t^2}\sum_{t=1}^{N_t}\sum_{n=1}^{N_t}\left(\boldsymbol{R}_{yx}\boldsymbol{R}_{yx}^H+\delta_{n,t}\mathrm{tr}\left(\boldsymbol{R}_{xx}\right)\boldsymbol{R}_{yy}\right)\\&=\Psi+\frac{1}{N_t}\mathrm{tr}\left(\boldsymbol{R}_{xx}\right)\boldsymbol{R}_{yy}\end{aligned} \tag{64}$$

where $\boldsymbol{e}_i$ denotes the $M\times 1$ vector having 1 at the ith position and zeros elsewhere. Similarly, from (6) and (9), we obtain

$$\begin{aligned}E\{\widehat{\overline{\Psi}}\}&=E\left\{\hat{\boldsymbol{R}}_{yx}\hat{\boldsymbol{R}}_{yx}^H+\boldsymbol{J}_M\hat{\boldsymbol{R}}_{yx}^{*}\hat{\boldsymbol{R}}_{yx}^T\boldsymbol{J}_M\right\}\\&=E\{\widehat{\Psi}\}+\boldsymbol{J}_M\left(\frac{1}{N_t^2}\sum_{t=1}^{N_t}\sum_{n=1}^{N_t}E\{\boldsymbol{y}^{*}(t)\boldsymbol{x}^T(t)\right.\\&\quad\left.\cdot\boldsymbol{x}^{*}(n)\boldsymbol{y}^T(n)\}\right)\boldsymbol{J}_M\\&=\overline{\Psi}+\frac{1}{N_t}\mathrm{tr}\left(\boldsymbol{R}_{xx}\right)\left(\boldsymbol{R}_{yy}+\boldsymbol{J}_M\boldsymbol{R}_{yy}^{*}\boldsymbol{J}_M\right).\end{aligned} \tag{65}$$

Moreover by adopting the proof of Lemma 1 in [69], we can find that the cost function $f_n(\alpha)$ in (22) converges to the true cost function $\overline{f}_n(\alpha)\triangleq\boldsymbol{a}^H(\alpha)\,\Pi_{\alpha n}\boldsymbol{a}(\alpha)$ w.p.1 and uniformly in α when $N_t\to\infty$, and hence the estimates $\{\hat{\alpha}_k\}$ of the elevation angles of noncoherent signals approach the true parameters $\{\alpha_k\}$ w.p.1 as $N_t\to\infty$ (cf. [9]), i.e., $\lim_{N_t\to\infty}\hat{\boldsymbol{A}}_n\to\boldsymbol{A}_n$. Further as it is well known that the estimated cross-covariance matrix $\hat{\boldsymbol{R}}_{yx}$ in (55) is consistent, from (23), we easily obtain $\lim_{N_t\to\infty}\widehat{\tilde{\boldsymbol{R}}}_{yx}\to\tilde{\boldsymbol{R}}_{yx}$. Hence the estimated oblique projector $\hat{\boldsymbol{E}}_{\mathcal{A}_n|\overline{\mathcal{A}}_c}$ calculated from the matrix $\hat{\boldsymbol{A}}_n$ and $\widehat{\tilde{\boldsymbol{R}}}_{yx}$ is also consistent as the number of snapshots tends to infinity, i.e., $\lim_{N_t\to\infty}\hat{\boldsymbol{E}}_{\mathcal{A}_n|\overline{\mathcal{A}}_c}\to\boldsymbol{E}_{\mathcal{A}_n|\overline{\mathcal{A}}_c}$, and consequently we get

$$E\left\{\left(\boldsymbol{I}_M-\hat{\boldsymbol{E}}_{\mathcal{A}_n|\overline{\mathcal{A}}_c}\right)\right\}=\boldsymbol{I}_M-\boldsymbol{E}_{\mathcal{A}_n|\overline{\mathcal{A}}_c}. \tag{66}$$

On the other hand, from (29), (30), (34), and (35), the sample cross-correlation matrix $\hat{\boldsymbol{R}}_{\tilde{y}x}$ and the estimated telescoping

matrix $\hat{\boldsymbol{T}}_m$ can be expressed as

$$\hat{\boldsymbol{R}}_{\tilde{y}x} = \frac{1}{N_t}\sum_{t=1}^{N_t} \widehat{\tilde{\boldsymbol{y}}}\,(t)\,\boldsymbol{x}^H\,(t) = \left(\boldsymbol{I}_M - \hat{\boldsymbol{E}}_{\mathcal{A}_n\,|\overline{\mathcal{A}}_c}\right)\hat{\boldsymbol{R}}_{yx} \quad (67)$$

$$\begin{aligned}\hat{\boldsymbol{T}}_m &= \left[\boldsymbol{F}_m^{(1)}\hat{\boldsymbol{R}}_{\tilde{y}x}, \boldsymbol{F}_m^{(2)}\hat{\boldsymbol{R}}_{\tilde{y}x}, \ldots, \boldsymbol{F}_m^{(m+1)}\hat{\boldsymbol{R}}_{\tilde{y}x}\right] \\ &= \boldsymbol{F}_m\left(\boldsymbol{I}_{m+1}\otimes\hat{\boldsymbol{R}}_{\tilde{y}x}\right). \end{aligned} \quad (68)$$

Then from (48), (66), and (67), we have

$$\begin{aligned}E\{\widehat{\Phi}_m\} &= E\{\hat{\boldsymbol{T}}_m\hat{\boldsymbol{T}}_m^H\} \\ &= \boldsymbol{F}_m\left\{\boldsymbol{I}_{m+1}\otimes\left(E\left\{\hat{\boldsymbol{R}}_{\tilde{y}x}\hat{\boldsymbol{R}}_{\tilde{y}x}^H\right\}\right)\right\}\boldsymbol{F}_m^H \end{aligned} \quad (69)$$

where

$$\begin{aligned}E\left\{\hat{\boldsymbol{R}}_{\tilde{y}x}\hat{\boldsymbol{R}}_{\tilde{y}x}^H\right\} = E\Big\{&\left(\boldsymbol{I}_M - \hat{\boldsymbol{E}}_{\mathcal{A}_n\,|\overline{\mathcal{A}}_c}\right)\left(\hat{\boldsymbol{R}}_{yx}\hat{\boldsymbol{R}}_{yx}^H\right) \\ &\cdot\left(\boldsymbol{I}_M - \hat{\boldsymbol{E}}_{\mathcal{A}_n\,|\overline{\mathcal{A}}_c}\right)^H\Big\}. \end{aligned} \quad (70)$$

Because the received signals $\{\boldsymbol{y}\,(t)\}$ and $\{\boldsymbol{x}\,(t)\}$ are temporally complex white Gaussian random processes under the basic assumptions and $\hat{\boldsymbol{R}}_{yx}\hat{\boldsymbol{R}}_{yx}^H$ in (70) is the time-average of the products $\boldsymbol{y}\,(t)\,\boldsymbol{x}^H\,(t)$ for $1 \le t \le N_t$, we can find that $\hat{\boldsymbol{E}}_{\mathcal{A}_n\,|\overline{\mathcal{A}}_c}$ in (70) tends to be "slowly" time-varying with respect to $\boldsymbol{y}\,(t)\,\boldsymbol{x}^H\,(t)$ (i.e., $\hat{\boldsymbol{R}}_{yx}$) and hence it is "almost" independent of $\hat{\boldsymbol{R}}_{yx}\hat{\boldsymbol{R}}_{yx}^H$ (cf. [70], [71]). Then, from (70), we can obtain

$$\begin{aligned}E\left\{\hat{\boldsymbol{R}}_{\tilde{y}x}\hat{\boldsymbol{R}}_{\tilde{y}x}^H\right\} \approx\; &E\left\{\left(\boldsymbol{I}_M - \hat{\boldsymbol{E}}_{\mathcal{A}_n\,|\overline{\mathcal{A}}_c}\right)\right\}E\left\{\left(\hat{\boldsymbol{R}}_{yx}\hat{\boldsymbol{R}}_{yx}^H\right)\right\} \\ &\cdot E\left\{\left(\boldsymbol{I}_M - \hat{\boldsymbol{E}}_{\mathcal{A}_n\,|\overline{\mathcal{A}}_c}\right)^H\right\}. \end{aligned} \quad (71)$$

Hence, from (64), (66), and (71), we have

$$\begin{aligned}E\{\hat{\boldsymbol{R}}_{\tilde{y}x}\hat{\boldsymbol{R}}_{\tilde{y}x}^H\} = &\left(\boldsymbol{I}_M - \boldsymbol{E}_{\mathcal{A}_n\,|\overline{\mathcal{A}}_c}\right)\left(\Psi + \frac{1}{N_t}\mathrm{tr}\,(\boldsymbol{R}_{xx})\,\boldsymbol{R}_{yy}\right) \\ &\cdot\left(\boldsymbol{I}_M - \boldsymbol{E}_{\mathcal{A}_n\,|\overline{\mathcal{A}}_c}\right)^H. \end{aligned} \quad (72)$$

By substituting (72) into (69) and after some straightforward manipulations, we can obtain

$$\begin{aligned}E\{\widehat{\Phi}_m\} = \Phi_m + \frac{1}{N_t}\mathrm{tr}\Big(\boldsymbol{R}_{xx}\Big)\boldsymbol{F}_m\Big\{\boldsymbol{I}_{m+1}\otimes\Big(&\left(\boldsymbol{I}_M - \boldsymbol{E}_{\mathcal{A}_n\,|\overline{\mathcal{A}}_c}\right) \\ &\cdot\boldsymbol{R}_{yy}\left(\boldsymbol{I}_M - \boldsymbol{E}_{\mathcal{A}_n\,|\overline{\mathcal{A}}_c}\right)^H\Big)\Big\}\boldsymbol{F}_m^H. \end{aligned} \quad (73)$$

Thus from (64), (65) and (73), the asymptotical errors $E\{\widehat{\Psi} - \Psi\}$, $E\{\widehat{\overline{\Psi}} - \overline{\Psi}\}$ and $E\{\widehat{\Phi}_m - \Phi_m\}$ in (58)–(60) can be obtained immediately. ■

Obviously from (58)–(60), we can see that the asymptotical errors of the estimates $\widehat{\Psi}$, $\widehat{\overline{\Psi}}$ and $\widehat{\Phi}_m$ approach zero w.p.1 as the number of snapshots N_t tends to infinity, i.e., $\widehat{\Psi} \to \Psi$, $\widehat{\overline{\Psi}} \to \overline{\Psi}$ and $\widehat{\Phi}_m \to \Phi_m$ almost sure (a.s.) as $N_t \to \infty$. Hence, from (10), (11), and (51)–(54), we can find that the estimated numbers of noncoherent and coherent signals are asymptotically consistent (cf. (Appendix C, [30])), i.e., $\hat{K}_n \to K_n, \hat{K}_p \to K_p$, and $\hat{P} \to P$ w.p.1 as $N_t \to \infty$. Thus as the number of snapshots N_t tends to infinity, the proposed OPEMS is consistent.

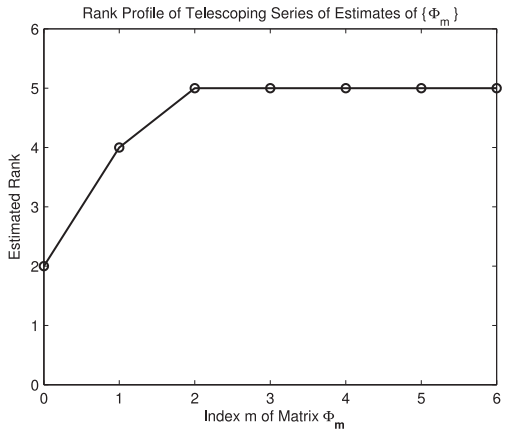

Fig. 5. The rank profile of the telescoping series of matrices in Example 1 ($M = 12, N_t = 128, \mathrm{SNR} = 5\,\mathrm{dB}, K_n = 2, K_1 = 2, K_2 = 3, K_c = 5,$ and $P = 2$).

V. Numerical Examples

Here we evaluate the performance of the proposed OPEMS in estimating the numbers of the noncoherent and coherent signals through numerical examples. The ULAs and sensors are separated by a half-wavelength, i.e., $d_x = d_y = \lambda/2$, and the SNR is defined as the ratio of the power of signal to that of the additive noise at each sensor. All of the simulation results shown below are based on 1000 independent trials, and the SRP test with the EVD-based MDL criterion [39], [17] is carried out for performance comparison, where the OPEMS for detection of the noncoherent and coherent signals are denoted as the OPEMS-NS and OPEMS-CS, while the SRP test for the detection of noncoherent and that of coherent signals are indicated as the SRP-NS and SRP-CS, respectively.

Example 1: We examine the detection performance of the proposed OPEMS in terms of the SNR. There are two noncoherent signals coming from (35°, 38°) and (45°, 65°) with correlation coefficient $0.3e^{-j\pi/18}$, while five coherent signals with two groups coming from (60°, 52°) and (82°, 93°) with attenuation coefficients $\boldsymbol{\eta}_1 = \left[1, e^{j\pi/6}\right]^T$ and (93°, 78°), (110°, 102°) and (130°, 20°) with attenuation coefficients $\boldsymbol{\eta}_2 = \left[1, e^{-j\pi/12}, e^{j\pi/4}\right]^T$, where $K_n = 2, P = 2, K_1 = 2, K_2 = 3,$ and $K_c = 5$. The number of sensors in one ULA is fixed at $M = 12$, and the number of snapshots is set as $N_t = 128$.

Firstly we inspect the ranks of the telescoping series of matrices $\{\widehat{\Phi}_m\}$ obtained in Step 6 of the OPEMS implementation. When $\mathrm{SNR} = 5$ dB, the rank profile of $\widehat{\Phi}_m$ in one independent trial is illustrated in Fig. 5, where $m = 0, 1, \ldots, M - K_c - 1$, and $M - K_c - 1 = 6$. Obviously we can see that the rank profile has two segments: the increasing segment at $m = 0, 1, 2$, where the rank increases monotonically with the unfolding of the deflated signal subspace due to the coherence of some incident signals (cf. [39]), and the stationary segment at $m = 2, 3, \ldots, 6$, where the rank becomes stationary since the entire subspace is fully restored. Then from (51)–(54) and Remark 3, we can obtain $\overline{M} = \hat{L} = 3, \hat{K}_c = 5, \hat{g}_2 = 1,$ and $\hat{g}_3 = 1$. As a result, from the source coherency structure $\{\hat{g}_l\}_{l=2}^3$, we can find that there are one group of two coherent signals and one of three coherent signals, i.e.,

$$\{\hat{K}_1, \hat{K}_2\} = \{\underbrace{2}_{\hat{g}_2}, \underbrace{3}_{\hat{g}_3}\}. \quad (74)$$

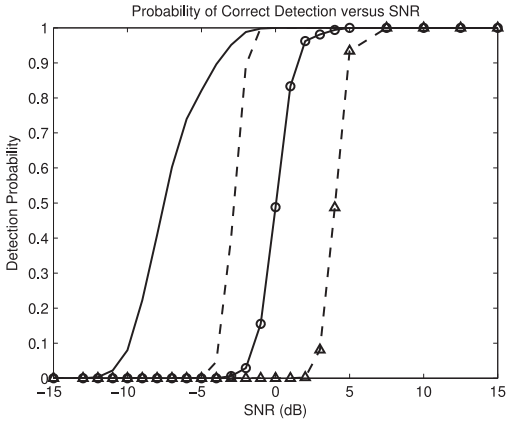

Fig. 6. The probability of correct detection versus the SNR (dashed line: SRP-NS; dashed line with "△": SRP-CS; solid line: OPEMS-NS; and solid line with "o": OPEMS-CS) in Example 1 ($M = 12, N_t = 128, K_n = 2, K_1 = 2, K_2 = 3, K_c = 5$, and $P = 2$).

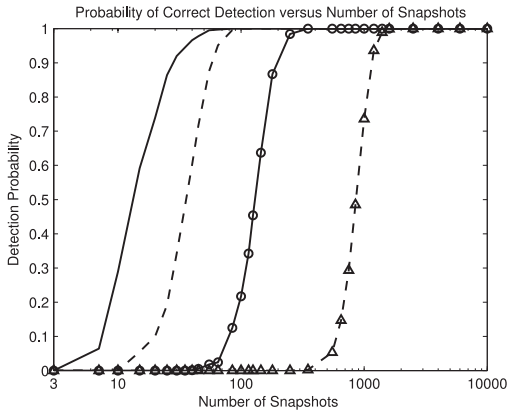

Fig. 7. The probability of correct detection versus the number of snapshots (dashed line: SRP-NS; dashed line with "△": SRP-CS; solid line: OPEMS-NS; and solid line with "o": OPEMS-CS) in Example 2 ($M = 12, \mathrm{SNR} = 0$ dB, $K_n = 2, K_1 = 2, K_2 = 3, K_c = 5$, and $P = 2$).

Hence the number of coherent signals in each group (i.e., the source coherency structure) can be estimated correctly.

Fig. 6 shows the probabilities of correct detection of the proposed OPEMS and the SRP method versus the SNR for the noncoherent signals and the coherent signals with multiple groups, while the SNR is varied from -15 to 15 dB. The SRP test can estimate the numbers of noncoherent and coherent signals (i.e., K_n, K_1, and K_2) together, but it performs poor at low and medium SNRs owing to the bias in the eigenvalue estimation. Since the influence of additive noises is mitigated by using the cross-correlations between the noisy data of two ULAs and the oblique projector is utilized to isolate the coherent signals from the noncoherent ones, the proposed OPEMS can estimate the numbers of noncoherent and coherent signals independently, and it outperforms the SRP test, where the computationally cumbersome eigendecomposition is not needed.

Example 2: Then we test the detection performance versus the number of snapshots. The simulation conditions are similar to that in Example 1, except that the SNR is fixed at 0 dB, and the number of snapshots N_t is varied from 3 to 10000.

The probabilities of correct detection of the proposed OPEMS and the SRP test in terms of the number of snapshots are shown in Fig. 7. When the number of snapshots is relatively small, the estimated eigenvalues of array covariance matrix become inaccurate, and hence it cause the degraded detection performance with the SRP test. However, since the numbers of noncoherent and coherent signals are determined respectively with the aid of the cross-correlations of noisy array data and the oblique projector, the proposed OPEMS provides better detection performance than the SRP method with small number of snapshots.

Example 3: Now we assess the detection performance in terms of the angular separation between the noncoherent and coherent signals. There are one uncorrelated signal coming from $(\alpha_1, 40^\circ)$ and two coherent signals from $(65^\circ, 70^\circ)$ and $(\alpha_3, 55^\circ)$ with the attenuation coefficients $\boldsymbol{\eta}_1 = [1, e^{j\pi/6}]^T$, where $\alpha_1 = \alpha_3 + \Delta\alpha, \alpha_3 = 85^\circ$, and $\Delta\alpha$ is varied from 1° to 15°. The number of sensors in one ULA is $M = 7$, and the number of snapshots is fixed as $N_t = 128$, while the SNR is set at 2.5 dB.

The probability of correct detection against the angular separation is plotted in Fig. 8. Since the SRP test estimates the number of noncoherent signals and that of coherent ones simultaneously, it has difficulty to distinguish the closely-spaced noncoherent and coherent signals. Hence the SRP method has lower detection probability for small angular separations. However, the proposed OPEMS isolates the coherent signals from the noncoherent one with the oblique projector, and consequently it is of advantage to resolve the closely-spaced noncoherent and coherent signals for small angular separations in this empirical scenario (the difference between the OPEMS-NS and OPEMS-CS is almost indistinguishable).

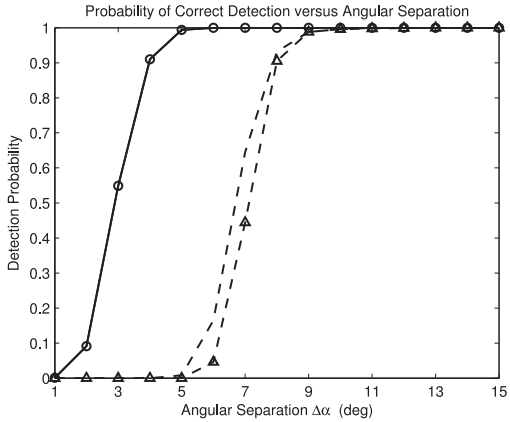

Fig. 8. The probability of correct detection in terms of the angular separation (dashed line: SRP-NS; dashed line with "△": SRP-CS; solid line: OPEMS-NS; and solid line with "o": OPEMS-CS) in Example 3 ($M = 7, N_t = 128, \mathrm{SNR} = 2.5$ dB, $K_n = 1, K_1 = 2, K_c = 2$, and $P = 1$).

Example 4: Finally we validate the resolvability of the proposed OPEMS versus the SNR with relatively less number of sensors. There are one uncorrelated signals coming from (35°, 38°) and two correlated signals from (40°, 65°) and (55°, 52°) with correlation coefficient $0.3e^{-j\pi/18}$, while seven coherent signals with three groups from (75°, 93°) and (86°, 78°) with attenuation coefficients $\boldsymbol{\eta}_1 = [1, e^{j\pi/6}]^T$, (94°, 102°) and (105°, 20°) with attenuation coefficients $\boldsymbol{\eta}_2 = [1, e^{-j\pi/3}]^T$, and (114°, 140°), (130°, 100°) and (150°, 125°) with attenuation coefficients $\boldsymbol{\eta}_3 = [1, e^{-j\pi/12}, e^{j\pi/4}]^T$. Herein $K_n = 3, P = 3, K_1 = 2, K_2 = 2, K_3 = 3$, and $K_c = \sum_{p=1}^{P} K_p = 7$. Additionally the number of snapshots is set as $N_t = 128$.

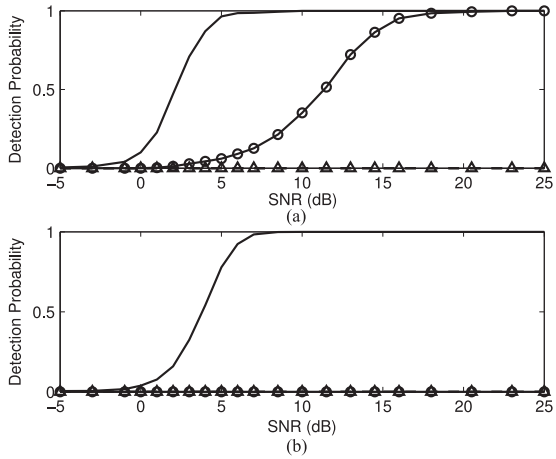

Fig. 9. The probability of correct detection versus SNR with different numbers of sensors (dashed line: SRP-NS; dashed line with "△": SRP-CS; solid line: OPEMS-NS; and solid line with "o": OPEMS-CS) in Example 4 ($N_t = 128, K_n = 3, K_1 = 2, K_2 = 2, K_3 = 3, K_c = 7$, and $P = 3$). (a) Probability of Correct Detection versus SNR $(\mathrm{M} = 11)$, (b) Probability of Correct Detection versus SNR $(\mathrm{M} = 10)$.

As analyzed in Remark 6, the minimum numbers of sensors required by the proposed OPEMS and the SRP test are $M_{\mathrm{OPEMS}} = 11$ and $M_{\mathrm{SRP}} = 14$, respectively. Fig. 9(a) depicts the detection performance in terms of the SNR, when the number of sensors in one ULA is set as $M = 11$. Evidently the proposed OPEMS can estimate the numbers of noncoherent and coherent signals separately even the number of sensors equals to the least necessary number of sensors (i.e., $M = M_{\mathrm{OPEMS}} = 11$), however the SRP test fails to estimate the numbers of signals duo to $M < M_{\mathrm{SRP}} = 14$. Clearly for the fixed number of incident signals, the proposed OPEMS needs less array sensors and has stronger detection capability compared to the SRP test. Moreover, Fig. 9(b) exhibits the corresponding detection performance for $M = 10$. Although the proposed OPEMS does not success to estimate the number of coherent signals similar to the SRP test due to the facts $M < M_{\mathrm{OPEMS}}$ and $M < M_{\mathrm{SRP}}$, it still has capability to estimate the number of noncoherent signals correctly at higher SNRs, because the number of noncoherent signals and that of coherent signals are estimated independently, where $M > K_n + 2P$. Unfortunately, the SRP test also fails to determine the number of noncoherent signals, because it can not estimate the number of noncoherent signals and that of coherent signals separately.

VI. Conclusion

In this paper, a new enumeration method without eigendecomposition called OPEMS was proposed for determining the number of noncoherent signals and that of coherent signals with multiple groups impinging on two parallel ULAs. With the aid of oblique projector, the number of noncoherent signals and that of coherent signals in each group are estimated separately, where only elevation angles of noncoherent signals are estimated, and the computationally intensive eigendecomposition procedure is avoided in the number detection and DOA estimation. The consistency of the OPEMS was analyzed, and its effectiveness was verified through numerical examples. The simulation results demonstrated that the OPEMS has good performance in detecting the numbers of noncoherent and coherent signals with a small number of snapshots and/or at relatively low SNR and can detect more incident signals.

Appendix A
QR-Based Rank Determination

For a square matrix $\overline{\Phi}$ with dimension $M \times M$ and rank p, i.e., $\rho\left(\overline{\Phi}\right) = p$, where $p < M$, its QR decomposition with column pivoting is given by (e.g., [45], [30])

$$\overline{\Phi\Pi} = \overline{\boldsymbol{Q}\boldsymbol{R}} = \overline{\boldsymbol{Q}} \begin{bmatrix} \overline{\boldsymbol{R}}_{11} & \overline{\boldsymbol{R}}_{12} \\ \boldsymbol{O}_{(M-p)\times M} \end{bmatrix} \begin{matrix} \}p \\ \}M-p \end{matrix} \tag{A1}$$

where $\overline{\Pi}$ is the $M \times M$ permutation matrix, $\overline{\boldsymbol{Q}}$ is the $M \times M$ unitary matrix, $\overline{\boldsymbol{R}}_{11}$ is the $p \times p$ upper triangular and nonsingular matrix, and $\overline{\boldsymbol{R}}_{12}$ is the $p \times (M-p)$ nonzero matrix. Clearly we have $\rho\left(\overline{\Phi}\right) = \rho\left(\overline{\boldsymbol{R}}\right) = p$. In a similar way to [30], by introducing an auxiliary quantity $\zeta(i)$ in terms of the elements of the ith row of QR factor $\overline{\boldsymbol{R}}$ as

$$\zeta(i) \triangleq \sum_{k=1}^{M} |\overline{r}_{ik}| + \epsilon = \overline{\zeta}_i + \epsilon, \text{for } i = 1, 2, \ldots, M \tag{A2}$$

where $\overline{\zeta}_i \triangleq \sum_{k=1}^{M} |\overline{r}_{ik}|$, and ϵ is an arbitrary and positive small constant (e.g., $\epsilon = 10^{-6}$), we can define the QRRC for the matrix $\overline{\Phi}$ as

$$\mathrm{QRRC}_{\overline{\Phi}}(i) \triangleq \frac{\zeta(i)}{\zeta(i+1)}, \text{for } i = 1, 2, \ldots, M-1. \tag{A3}$$

Then the ratio criterion $\mathrm{QRRC}_{\overline{\Phi}}(i)$ can be expressed as

$$\mathrm{QRRC}_{\overline{\Phi}}(i) \tag{A4}$$

$$= \begin{cases} \frac{\overline{\zeta}_i + \epsilon}{\overline{\zeta}_{i+1} + \epsilon} \approx \frac{\overline{\zeta}_i}{\overline{\zeta}_{i+1}} \triangleq c(i), & \text{for } 1 \le i < p \\ \frac{\overline{\zeta}_n + \epsilon}{\epsilon} \to \infty, & \text{for } i = p \\ \frac{\epsilon}{\epsilon} = 1, & \text{for } p < i \le M-1 \end{cases} \tag{A5}$$

Thus the rank p is determined as the value of the running index $i \in \{1, \ldots, M-1\}$ for which the criterion $\mathrm{QRRC}_{\overline{\Phi}}(i)$ is maximized, i.e.,

$$p = \underset{i \in \{1,\ldots,M-1\}}{\arg\max}\ \mathrm{QRRC}_{\overline{\Phi}}(i). \tag{A5}$$

■

Acknowledgment

The authors would like to thank the anonymous reviewers and the associate editor Prof. Adel Belouchrani for their careful review, insightful comments, and valuable suggestions.

References

[1] H. Krim and M. Viberg, "Two decades of array signal processing research: The parametric approach," *IEEE Signal Process. Mag.*, vol. 13, no. 4, pp. 67–94, 1996.

[2] H. L. Van Trees, *Optimum Array Processing, Part IV of Detection, Estimation, and Modulation Theory*, New York, NY, USA: Wiley, 2002.

[3] R. O. Schmidt, "Multiple emitter location and signal parameter estimation," in *Proc. RADC Spectrum Estimation Workshop*, Rome, NY, USA, Oct. 1979, pp. 243–258.

[4] R. Kumaresan and D. W. Tufts, "Estimating the angles of arrival of multiple plane waves," *IEEE Trans. Aerosp. Electron. Syst.*, vol. 19, no. 1, pp. 134–139, 1983.

[5] R. Roy and T. Kailath, "ESPRIT—Estimation of signal parameters via rotational invariance techniques," *IEEE Trans. Acoust., Speech, Signal Process.*, vol. 37, no. 7, pp. 984–995, 1989.

[6] P. Stoica and K. C. Sharman, "Novel eigenanalysis method for direction estimation," *Proc. Inst. Electr. Eng.–F*, vol. 137, no. 1, pp. 19–26, 1990.

[7] A. Eriksson, P. Stoica, and T. Söderström, "On-line subspace algorithms for tracking moving sources," *IEEE Trans. Signal Process.*, vol. 42, no. 9, pp. 2319–2330, 1994.

[8] S. Marcos, A. Marsal, and M. Benidir, "The propagator method for source bearing estimation," *Signal Process.*, vol. 42, pp. 121–138, 1995.

[9] J. Xin and A. Sano, "Computationally efficient subspace-based method for direction-of-arrival estimation without eigendecomposition," *IEEE Trans. Signal Process.*, vol. 52, no. 4, pp. 876–893, 2004.

[10] N. Yuen and B. Friedlander, "DOA estimation in multipath: An approach using fourth-order cumulants," *IEEE Trans. Signal Process.*, vol. 45, no. 5, pp. 1253–1263, 1997.

[11] E. Gönen and J. M. Mendel, "Applications of cumulants to array processing—Part III: Blind beamforming for coherent signals," *IEEE Trans. Signal Process.*, vol. 45, no. 9, pp. 2252–2264, 1997.

[12] E. Gönen, J. M. Mendel, and M. C. Dogăn, "Applications of cumulants to array processing—Part IV: Direction finding in coherent signals case," *IEEE Trans. Signal Process.*, vol. 45, no. 9, pp. 2265–2276, 1997.

[13] Y.-M. Chen, "On spatial smoothing for two-dimensional direction-of-arrival estimation of coherent signals," *IEEE Trans. Signal Process.*, vol. 45, no. 7, pp. 1689–1696, 1997.

[14] H. Wang and K. J. R. Liu, "2-D spatial smoothing for multipath coherent signal separation," *IEEE Trans. Aerosp. Electron. Syst.*, vol. 34, no. 2, pp. 391–405, 1998.

[15] G. Wang, J. Xin, N. Zheng, and A. Sano, "Computationally efficient subspace-based method for two-dimensional direction estimation with L-shaped array," *IEEE Trans. Signal Process.*, vol. 59, no. 7, pp. 3197–3212, 2011.

[16] H. Tao, J. Xin, J. Wang, N. Zheng, and A. Sano, "Two-dimensional direction estimation for a mixture of noncoherent and coherent signals," *IEEE Trans. Signal Process.*, vol. 63, no. 2, pp. 318–333, 2015.

[17] M. Wax and T. Kailath, "Detection of signals by information theoretic criteria," *IEEE Trans. Acoust., Speech, Signal Process.*, vol. 33, no. 2, pp. 387–392, 1985.

[18] P. Stoica and Y. Selen, "Model-order selection: A review of information criterion rules," *IEEE Signal Process. Mag.*, vol. 21, no. 4, pp. 36–47, 2004.

[19] E. Fishler and H. V. Poor, "Estimation of the number of sources in unbalanced arrays via information theoretic criteria," *IEEE Trans. Signal Process.*, vol. 53, no. 9, pp. 3543–3553, 2005.

[20] Z. Lu and A. M. Zoubir, "Generalized Bayesian information criterion for source enumeration in array processing," *IEEE Trans. Signal Process.*, vol. 61, no. 6, pp. 1470–1480, 2013.

[21] W. Chen, K. M. Wong, and J. P. Reilly, "Detection of the number of signals: A predicted eigen-threshold," *IEEE Trans. Signal Process.*, vol. 39, no. 5, pp. 1088–1098, 1991.

[22] H. Lee and F. Li, "An eigenvector technique for detecting the number of emitters in a cluster," *IEEE Trans. Signal Process.*, vol. 42, no. 9, pp. 2380–2388, 1994.

[23] H.-T. Wu, J.-F. Yang, and F.-K. Chen, "Source number estimators using transformed Gerschgorin radii," *IEEE Trans. Signal Process.*, vol. 43, no. 6, pp. 1325–1333, 1995.

[24] R. F. Brcich, A. M. Zoubir, and P. Pelin, "Detection of sources using bootstrap techniques," *IEEE Trans. Signal Process.*, vol. 50, no. 2, pp. 206–215, 2002.

[25] A. Di, "Multiple source location—A matrix decomposition approach," *IEEE Trans. Acoust., Speech, Signal Process.*, vol. 33, no. 4, pp. 1086–1091, 1985.

[26] G. Xu, R. H. RoyIII, and T. Kailath, "Detection of number of sources via exploitation of centro-symmetry property," *IEEE Trans. Signal Process.*, vol. 42, no. 1, pp. 102–112, 1994.

[27] J. H. Cozzens and M. J. Sousa, "Source enumeration in a correlated signal environment," *IEEE Trans. Signal Process.*, vol. 42, no. 2, pp. 304–317, 1994.

[28] H. Krim and J. H. Cozzens, "A data-based enumeration technique for fully correlated signals," *IEEE Trans. Signal Process.*, vol. 42, no. 7, pp. 1662–1668, 1994.

[29] P. J. Green and D. P. Taylor, "Dynamic signal enumeration algorithm for smart antennas," *IEEE Trans. Signal Process.*, vol. 50, no. 6, pp. 1307–1314, 2002.

[30] J. Xin, N. Zheng, and A. Sano, "Simple and efficient nonparametric method for estimating the number of signals without eigendecomposition," *IEEE Trans. Signal Process.*, vol. 55, no. 4, pp. 1405–1418, 2007.

[31] M. Wax and I. Ziskind, "Detection of the number of coherent signals by the MDL principle," *IEEE Trans. Acoust., Speech, Signal Process.*, vol. 37, no. 8, pp. 1190–1196, 1989.

[32] Q. Wu and D. R. Fuhrmann, "A parametric method for determining the number of signals in narrow-band direction finding," *IEEE Trans. Signal Process.*, vol. 39, no. 8, pp. 1848–1857, 1991.

[33] M. Wax, "Detection and localization of multiple sources via the stochastic signals model," *IEEE Trans. Signal Process.*, vol. 39, no. 11, pp. 2450–2456, 1991.

[34] M. Viberg, B. Ottersten, and T. Kailath, "Detection and estimation in sensor arrays using weighted subspace fitting," *IEEE Trans. Signal Process.*, vol. 39, no. 11, pp. 2436–2449, 1991.

[35] R. E. Bethel and K. L. Bell, "Maximum likelihood approach to joint array detection/estimation," *IEEE Trans. Aerosp. Electron. Syst.*, vol. 40, no. 3, pp. 1060–1072, 2004.

[36] S. Valaee and P. Kabal, "An information theoretic approach to source enumeration in array signal processing," *IEEE Trans. Signal Process.*, vol. 52, no. 5, pp. 1171–1178, 2004.

[37] P.-J. Chung, J. F. Böhme, C. F. Mecklenbrauker, and A. O. Hero, "Detection of the number of signals using the Benjamini-Hochberg procedure," *IEEE Trans. Signal Process.*, vol. 55, no. 6, pp. 2497–2508, 2007.

[38] J. A. Cadzow, "A high resolution direction-of-arrival algorithm for narrow-band coherent and incoherent sources," *IEEE Trans. Acoust., Speech, Signal Process.*, vol. 36, no. 7, pp. 965–979, 1988.

[39] T.-J. Shan, A. Paulraj, and T. Kailath, "On smoothed rank profile tests in eigenstructure methods for directions-of-arrival estimation," *IEEE Trans. Acoust., Speech, Signal Process.*, vol. 35, no. 10, pp. 1377–1385, 1987.

[40] S. Prasad and B. Chandna, "An augmented smoothed rank profile algorithm for determination of source coherency structure," *IEEE Trans. Acoust., Speech, Signal Process.*, vol. 37, no. 7, pp. 1144–1146, 1989.

[41] Z. Ye, Y. Zhang, and C. Liu, "Direction-of-arrival estimation for uncorrelated and coherent signals with fewer sensors," *IET Microw. Antennas Propag.*, vol. 3, no. 3, pp. 473–482, 2009.

[42] T.-J. Shan, M. Wax, and T. Kailath, "On spatial smoothing of estimation of coherent signals," *IEEE Trans. Acoust., Speech, Signal Process.*, vol. 33, no. 4, pp. 806–811, 1985.

[43] S. U. Pillai and B. H. Kwon, "Forward/backward spatial smoothing techniques for coherent signals identification," *IEEE Trans. Acoust., Speech, Signal Process.*, vol. 37, no. 1, pp. 8–15, 1989.

[44] R. T. Williams, S. Prasad, A. K. Mahalanabis, and L. H. Sibul, "An improved spatial smoothing technique for bearing estimation in a multipath environment," *IEEE Trans. Acoust., Speech, Signal Process.*, vol. 36, no. 4, pp. 425–432, 1988.

[45] G. H. Golub and C. F. Van Loan, *Matrix Computations*, 2nd, Baltimore, MD, USA: The John Hopkins Univ. Press, 1989.

[46] S. Haykin, *Adaptive Filter Theory*, 4th, Englewood Cliffs, NJ, USA: Prentice-Hall, 2002.

[47] P. Comon and G. H. Golub, "Tracking a few extreme singular values and vectors in signal processing," *Proc. IEEE*, vol. 78, no. 8, pp. 1327–1343, 1990.

[48] J. P. Reilly and M. K. Law, "A fast high-performance array processing technique for angle-of-arrival estimation and detection of the number of incident signals," *Can. J. Elect. Comput. Eng.*, vol. 14, no. 2, pp. 8–45, 1989.

[49] J. P. Reilly, "A real-time high-resolution technique for angle-of-arrival estimation," *Proc. IEEE*, vol. 75, no. 12, pp. 1692–1694, 1987.

[50] P. Comon, L. Kopp, and J. P. Reilly, "Comments, with reply, on "A real-time high-resolution technique for angle-of-arrival estimation," *Proc. IEEE*, vol. 77, no. 3, pp. 492–494, 1989.

[51] L. Huang, T. Long, and S. Wu, "Source enumeration for high-resolution array processing using improved Gerschgorin radii without eigendecomposition," *IEEE Trans. Signal Process.*, vol. 56, no. 12, pp. 5916–5925, 2008.

[52] L. Huang, T. Long, E. Mao, and H. C. So, "MMSE-based MDL method for robust estimation of number of sources without eigendecomposition," *IEEE Trans. Signal Process.*, vol. 57, no. 10, pp. 4135–4142, 2009.

[53] H. Tao, J. Xin, J. Wang, N. Zheng, and A. Sano, "Estimation of the number of narrowband signals in the presence of multipath propagation," in *Proc. IEEE 7th Sens. Array Multichannel Signal Process. Workshop*, Hoboken, NJ, USA, Jun. 2012, pp. 497–500.

[54] A. L. Swindlehurst, P. Stoica, and M. Jansson, "Exploiting arrays with multiple invariances using MUSIC and MODE," *IEEE Trans. Signal Process.*, vol. 49, no. 11, pp. 2511–2521, 2001.

[55] Y. Hua, T. K. Sarkar, and D. D. Weiner, "An L-shaped array for estimating 2-D directions of wave arrival," *IEEE Trans. Antennas Propag.*, vol. 39, no. 2, pp. 143–146, 1991.

[56] Q. Y. Yin, R. W. Newcomb, and L. H. Zou, "Estimating 2-D angles of arrival via two parallel linear arrays," in *Proc. IEEE Int. Conf. Acoust., Speech, Signal Process.*, Glasgow, U.K., May 1989, pp. 2803–2806.

[57] N. Tayem and H. M. Kwon, "L-shape 2-dimensional arrival angle estimation with propagator method," *IEEE Trans. Antennas Propag.*, vol. 53, no. 5, pp. 1622–1630, 2005.

[58] T. Xia, Y. Zheng, Q. Wan, and X. Wang, "Decoupled estimation of 2-D angles of arrival using two parallel uniform linear arrays," *IEEE Trans. Antennas Propag.*, vol. 55, no. 9, pp. 2627–2632, 2007.
[59] G. Wang, J. Xin, J. Wang, N. Zheng, and A. Sano, "Subspace-based two-dimensional direction estimation and tracking of multiple targets," *IEEE Trans. Aerosp. Electron. Syst.*, vol. 51, no. 2, pp. 1386–1402, 2015.
[60] R. T. Behrens and L. L. Scharf, "Signal processing application of oblique projection operators," *IEEE Trans. Signal Process.*, vol. 42, no. 6, pp. 1413–1424, 1994.
[61] D. A. Linebarger, R. D. DeGroat, and E. M. Dowling, "Efficient direction-finding methods employing forward/backward averaging," *IEEE Trans. Signal Process.*, vol. 42, no. 8, pp. 2136–2145, 1994.
[62] W. M. Gentleman and H. T. Kung, "Matrix triangularization by systolic arrays," in *Proc. SPIE, Real-Time Signal Process. IV*, 1981, vol. 298, pp. 19–26.
[63] P. H. Ang and M. Morf, "Concurrent array processor for fast eigenvalue computations," in *Proc. IEEE Int. Conf. Acoust., Speech, Signal Process.*, San Diego, CA, USA, Mar. 1984, vol. 9, pp. 766–769.
[64] J. P. Reilly, W. G. Chen, and K. M. Wong, "A fast QR-based array-processing algorithm," in *Proc. SPIE, Adva. Algorithms Architect. Signal Process. III*, 1988, vol. 975, pp. 36–47.
[65] J. Reilly, J. Litva, and P. Bauman, "New angle-of-arrival estimator: Comparative evaluation applied to the low-angle tracking radar problem," *Proc. Inst. Electr. Eng.—F*, vol. 135, no. 5, pp. 408–420, 1988.
[66] G. A. Sitton, C. S. Burrus, J. W. Fox, and S. Treitel, "Factoring very-high-degree polynomials," *IEEE Signal Process. Mag.*, vol. 20, no. 6, pp. 27–42, 2003.
[67] Y. Zhang, Z. Ye, X. Xu, and J. Cui, "Estimation of two-dimensional direction-of-arrival for uncorrelated and coherent signals with low complexity," *IET Radar Sonar Navig.*, vol. 4, no. 4, pp. 507–519, 2010.
[68] P. H. M. Janssen and P. Stoica, "On the expectation of the product of four matrix-valued Gaussian random variables," *IEEE Trans. Autom. Control*, vol. 33, no. 9, pp. 867–870, 1988.
[69] P. Stoica and T. Söderström, "Statistical analysis of a subspace method for bearing estimation without eigendecomposition," *Proc. Inst. Electr. Eng.—F*, vol. 139, no. 4, pp. 301–305, 1992.
[70] C. G. Samson and V. U. Reddy, "Fixed point error analysis of the normalized ladder algorithm," *IEEE Trans. Acoust., Speech, Signal Process.*, vol. 31, no. 5, pp. 1177–1191, 1983.
[71] J. Xin, N. Zheng, and A. Sano, "Subspace-based adaptive method for estimating direction-of-arrival with Luenberger observer," *IEEE Trans. Signal Process.*, vol. 59, no. 1, pp. 145–159, 2011.

Hao Tao received the B.E. and Ph.D. degrees in control science and engineering from Xi'an Jiaotong University, Xi'an, China, in 2009 and 2015, respectively.

He joined China Ship Development and Design Center in 2015, and his current research interests include array and statistical signal processing and adaptive control.

Jingmin Xin (S'92–M'96–SM'06) received the B.E. degree in information and control engineering from Xi'an Jiaotong University, Xi'an, China, in 1988 and the M.S. and Ph.D. degrees in electrical engineering from Keio University, Yokohama, Japan, in 1993 and 1996, respectively.

From 1988 to 1990, he was with the Tenth Institute of Ministry of Posts and Telecommunications (MPT) of China, Xi'an. He was with the Communications Research Laboratory, MPT of Japan, as an Invited Research Fellow of the Telecommunications Advancement Organization of Japan (TAO) from 1996 to 1997 and as a Postdoctoral Fellow of the Japan Science and Technology Corporation (JST) from 1997 to 1999. He was also a Guest (Senior) Researcher with YRP Mobile Telecommunications Key Technology Research Laboratories Company, Limited, Yokosuka, Japan, from 1999 to 2001. From 2002 to 2007, he was with Fujitsu Laboratories Limited, Yokosuka, Japan. Since 2007, he has been a Professor at Xi'an Jiaotong University.

His research interests are in the areas of adaptive filtering, statistical and array signal processing, system identification, and pattern recognition.

Jiasong Wang graduated from Astronomy department, Nanjing University, China in 1990, and received the M.S. degree in satellite orbit dynamics from Nanjing University in 1996 and the Ph.D. degree in civil engineering and geosciences from Newcastle University, U.K. in 2004.

He joined Xi'an Satellite Control Center in 1990, and is currently a research fellow and vice director of the State Key Laboratory of Astronautic Dynamics in China. His research concentrates on satellite orbit determination, precise satellite navigation, space geodesy and geophysical inferences from satellite orbit perturbations.

Dr. Wang has been a member of orbit expert panel for Chinese manned spaceflight engineering since 2007 and a member of expert group for Chinese high resolution earth observation project since 2011.

Nanning Zheng (SM'93–F'06) graduated from the Department of Electrical Engineering, Xi'an Jiaotong University, Xi'an, China, in 1975, and received the M.S. degree in information and control engineering from Xi'an Jiaotong University in 1981 and the Ph.D. degree in electrical engineering from Keio University, Yokohama, Japan, in 1985.

He jointed Xi'an Jiaotong University in 1975, and he is currently a Professor and the Director of the Institute of Artificial Intelligence and Robotics, Xi'an Jiaotong University. His research interests include computer vision, pattern recognition and image processing, and hardware implementation of intelligent systems.

Dr. Zheng became a member of the Chinese Academy of Engineering in 1999, and he is the Chinese Representative on the Governing Board of the International Association for Pattern Recognition. He also serves as the President of Chinese Association of Automation.

Akira Sano (M'89) received the B.E., M.S. and Ph.D. degrees in mathematical engineering and information physics from the University of Tokyo, Japan, in 1966, 1968 and 1971, respectively.

In 1971, he joined the Department of Electrical Engineering, Keio University, Yokohama, Japan, where he was a Professor with the Department of System Design Engineering till 2009, and he is currently Professor Emeritus of Keio University. He is a member of Science Council of Japan since 2005. He was a Visiting Research Fellow at the University of Salford, Salford, U.K., from 1977 to 1978. His current research interests are in adaptive modeling and design theory in control, signal processing and communication, and applications to control of sounds and vibrations, mechanical systems and mobile communication systems. He is a coauthor of the textbook *State Variable Methods in Automatic Control* (New York: Wiley, 1988).

Dr. Sano received the Kelvin Premium from the Institute of Electrical Engineering in 1986. He is a Fellow of the Society of Instrument and Control Engineers and is a Member of the Institute of Electrical Engineering of Japan and the Institute of Electronics, Information and Communications Engineers of Japan. He was General Co-chair of 1999 IEEE Conference of Control Applications and an IPC Chair of 2004 IFAC Workshop on Adaptation and Learning in Control and Signal Processing. He served as Chair of IFAC Technical Committee on Modeling and Control of Environmental Systems from 1996 to 2001. He has also been Vice Chair of IFAC Technical Committee on Adaptive Control and Learning since 1999 and has been Chair of IFAC Technical Committee on Adaptive and Learning Systems since 2002. He was also on the Editorial Board of *Signal Processing*.